

©Copyright by Shiyang Zhao 2015
All rights reserved

**SYNTHESIS AND CHARACTERIZATION OF ORGANIC MATERIALS
FOR AQUEOUS LITHIUM-ION BATTERIES**

A Thesis

Presented to

the Faculty of the Department of Electrical and Computer Engineering

University of Houston

In Partial Fulfillment

of the Requirements for the Degree

Master of Science

in Electrical Engineering

by

Shiyang Zhao

December 2015

**SYNTHESIS AND CHARACTERIZATION OF ORGANIC MATERIALS
FOR AQUEOUS LITHIUM-ION BATTERIES**

Shiyang Zhao

Approved:

Chair of the Committee
Dr. Yan Yao, Assistant Professor
Electrical and Computer Engineering

Committee Members:

Dr. Jiming Bao, Associate Professor
Electrical and Computer Engineering

Dr. Haleh Ardebili, Assistant Professor
Mechanical Engineering

Dr. Suresh K. Khator,
Associate Dean,
Cullen College of Engineering

Dr. Badrinath Roysam,
Professor and Department Chair,
Electrical and Computer Engineering

Acknowledgements

I would like to thank my advisor, Dr. Yan Yao, for his generous support to my master research. It is him who provided me this great opportunity to study and work in the lab even though I had little background knowledge in this field. During the two years' study in Dr. Yao's lab, I was impressed by his inspiring insights as well as his working attitude. I learned not only how to do research, appreciate the beauty of science, but also get to know what attitude should have to become successful. I will be benefited from these previous learning experiences in my whole life.

I would also like to express my deep gratitude to all group members, especially Yanliang Liang and Yan Jing, who has taught me every details of synthesis so patiently. They not only taught me why but also taught me the methods to solve problems independently. Without their help, I could not have completed my research within three semesters.

Finally, I want to thank my parents for their support during the tough period. They are the most important people to me, and I could not fulfill my academic goals without their continuous support and understanding during my study along the way. Also, I want to thank all of my friends, especially my roommate and boyfriend, who gave me a lot of strength and took care of me.

**SYNTHESIS AND CHARACTERIZATION OF ORGANIC MATERIALS
FOR AQUEOUS LITHIUM-ION BATTERIES**

An Abstract

of a

Thesis

Presented to

the Faculty of the Department of Electrical and Computer Engineering

University of Houston

In Partial Fulfillment

of the Requirements for the Degree

Master of Science

in Electrical Engineering

by

Shiyang Zhao

December 2015

Abstract

The world has never stopped seeking more sustainable and cost-effective lithium-ion batteries due to the increasing energy demand in the near future. Aqueous rechargeable lithium batteries (ARLBs) may become a viable candidate due to its excellent safety and reliability. Developing electroactive organic electrode materials for batteries have attracted more and more interests as green and low-cost materials. Among all these materials, polyimide materials with high mechanical strength and excellent thermal stability are particularly promising.

In this Master's research study, I have synthesized four imide-based materials and tested them in aqueous electrolyte as anode electrode materials. One of the four materials, N,N'-Bis(ethyl)-1,4,5,8-naphthalenetetracarboxylic diimide (NDIE), achieves a specific capacity of 121.3 mAh/g and a 57.7% capacity retention after 20 cycles. After the cell optimization, the capacity increased to 158.5 mAh/g and retention increased to 90%, respectively. The corresponding polymer, PNDIE, could achieve a specific capacity of 172.3 mAh/g and a 91.9% retention after 50 cycles. The excellent stability and high coulombic efficiency of PNDIE make it a promising anode electrode material candidate for ALIBs.

Table of Contents

Acknowledgements	v
Abstract	vii
Table of Contents	viii
List of Figures	xi
List of Tables	xv
Chapter 1 Introduction	1
1.1 Batteries and Other Energy Storage Devices	2
1.1.1 Brief History of Batteries	2
1.2 Lithium-ion Batteries	5
1.2.1 Basic Principles of Lithium-ion Battery	7
1.2.2 Typical Electrode Material	8
1.2.2.1 Traditional Anode Electrode Materials	8
1.2.2.2 Conventional Cathode Electrode Materials	10
1.2.3 Non-aqueous Liquid Electrolyte	11
1.3 Different Forms of Lithium-ion Batteries	12
1.4 Safety Issue in Non-aqueous Rechargeable Lithium Batteries	13
1.5 Background of Aqueous Rechargeable Lithium-ion Battery	14
1.6 Challenges in Aqueous Lithium-ion Batteries	16
Chapter 2 Literature Review	18
2.1 A Brief Review of Inorganic Electrode Materials in ARLBs	18
2.1.1 Cathode Materials	18

2.1.2	Anode Materials.....	21
2.2	A Brief Review of Organic Electrode Materials in ARLBs	23
2.2.1	Cathode Materials	24
2.2.2	Anode Materials.....	25
Chapter 3	Synthesis of Organic Materials	29
3.1	Materials Design	29
3.2	Equipment	30
3.3	Synthesis	34
3.3.1	Monomer.....	35
3.3.2	Polymer.....	37
3.3.3	Challenges for Monomer Synthesis.....	38
3.3.3.1	NDIE.....	39
3.3.3.2	PDIE.....	41
Chapter 4	Cell Fabrication and Characterization.....	43
4.1	Cell Fabrication and Electrode Preparation	43
4.1.1	Cell Fabrication	43
4.1.2	Electrode Preparation.....	44
4.2	Physical and Structure Characterizations.....	44
4.2.1	Nuclear Magnetic Resonance	44
4.2.2	Fourier Transform Infrared spectroscopy	45
4.2.3	Scanning Electron Microscope	47
4.3	Electrochemical Measurements	48
4.3.1	Cyclic Voltammetry (CV)	48

4.3.2 Galvanostatic Charge and Discharge Testing.....	49
4.3.2.1 Overall and Comparison Result	49
4.3.2.2 Progress of NDIE.....	51
4.3.2.3 Long Cycle Stability of PNDIE	53
4.3.2.4 Fast fading in PDIE's cycling life.....	55
Chapter 5 Conclusion and Summary	56
5.1 Conclusion	56
5.2 Summary	57
Bibliography.....	59

List of Figures

Figure 1.1 Structure of (a) a Baghdad battery and (b) a Daniell cell	3
Figure 1.2 Comparison between different rechargeable battery technologies in terms of volumetric and gravimetric energy densities	6
Figure 1.3 The lithium-ion battery mechanism.....	7
Figure 1.4 Voltage versus capacity for positive and negative electrode materials	8
Figure 1.5 (Left side) The structures of (a) Soft carbon (b) Hard carbon and (c) Graphite; (Right side) Their typical potential performances	9
Figure 1.6 Crystal structures of conventional cathode materials for lithium-ion batteries	11
Figure 1.7 Various lithium-ion battery configurations (a) Cylindrical (b) Coin (c) Prismatic and (d) Thin and flat	13
Figure 1.8 (Left side) O_2/H_2 evolution potential vs. NHE for different pH; (Right side) Intercalation potential of various lithium-ion electrode materials vs. NHE and Li/Li^+	15
Figure 2.1 (a) The discharge curves of the porous $LiMn_2O_4$ electrode (b) The cycling behaviors of the solid and porous $LiMn_2O_4$ electrodes	19
Figure 2.2 (a) Charge/discharge curves at different C-rates (b) Cycling performance at 7C of the as-prepared nano- $LiCoO_2$ in 0.5 mol/L Li_2SO_4 aqueous electrolytes.....	20
Figure 2.3 (a) Charge/discharge curves for the first cycle of $LiV_3O_8//LiCoO_2$ cells in organic and aqueous electrolytes (b) Cycling behavior of $LiV_3O_8//LiCoO_2$ in aqueous electrolytes at 1 C	21

Figure 2.4 (a) Cycling performance and coulombic efficiency curves of cell before coating PPy on bare anode (b) Charge/discharge curves of $\text{LiMn}_2\text{O}_4/\text{Li}_x\text{V}_2\text{O}_5\text{-PPy}$ cell (c) Cycling performance and coulombic efficiency curves of cell after coating PPy	22
Figure 2.5 (a) Cycling performance of the $\text{LiTi}_2(\text{PO}_4)_3/\text{LiMn}_2\text{O}_4$ aqueous lithium-ion battery at a current rate of 10 mA/cm^2 (b) CV curves of a $\text{LiTi}_2(\text{PO}_4)_3$ and LiMn_2O_4 at a sweep rate of 0.3 mV/s in $1 \text{ M Li}_2\text{SO}_4$ solution	23
Figure 2.6 Discharge capacity and coulombic efficiency for (a) AQ in $1 \text{ M LiTFSI/DOL} + \text{DME}$ electrolyte (b) AQ in $1 \text{ M LiClO}_4/\text{EC} + \text{DMC}$ electrolyte (c) PAQS in $1 \text{ M LiTFSI/DOL} + \text{DME}$ electrolyte	25
Figure 2.7 (a) Cycle performance of PVAQ (a') Charge/discharge curves of PVAQ (b) Charge/discharge curves of PVAQ/air cell (b') Cyclic voltammogram of the cell	26
Figure 2.8 (a) Charge/discharge curves for five polyimides under 0.1C (b) Cycle performance for five polyimides.....	26
Figure 2.9 Cycling performance of (a) NaVPO_4F and (b) Polyimide in 5 M NaNO_3 solution at a current density of 50 mA/g	27
Figure 2.10 Mechanism for reversible reduction of general carbonyl compounds	28
Figure 3.1 (a) Hot Plate (b) Tube Furnace (c) Rotary Evaporator (d) Vacuum Oven.....	31
Figure 3.2 (a) Precision Disc Cutter (b) Desk-Top Powder Presser (c) Analytical Balance (d) Fourier Transform Infrared Spectrometer (e) Handheld UV Lamps	32
Figure 3.3 (a) Compact Hydraulic Crimping Machine (b) Electric Crimper Machine (c) Glove Box Systems (d) Landhe Battery Testing System.....	33

Figure 3.4 PNDIE synthesis procedure.....	35
Figure 3.5 Imidization reaction mechanism.....	35
Figure 3.6 Electrochemical redox mechanisms	35
Figure 3.7 (a) NDIE (yield: 78.8%) (b) PDIE (yield: 20%)	36
Figure 3.8 Reaction equations for monomers	37
Figure 3.9 (a) PNDIE (yield: 85.9%) (b) PPDIE (yield: 73.8%).....	38
Figure 3.10 Reaction equations for PPDIE and PNDIE	38
Figure 3.11 Different attempts on 1-88 NDIE for improving the yield.....	40
Figure 3.12 Synthesis procedure for 1-99 NDIE	40
Figure 3.13 Information about the products from different position of sublimation chamber.....	41
Figure 3.14 Recrystallization procedure of 1-81 PDIE	42
Figure 4.1 Coin cell fabrication	43
Figure 4.2 NMR spectrum of NDIE and PDIE.....	45
Figure 4.3 IR spectroscopy of PNDIE, NDIE, PPDIE and PDIE.....	46
Figure 4.4 SEM Image of (a) NDIE (b) PDIE (c) PNDIE (d) PPDIE.....	47
Figure 4.5 Cyclic voltammetry of NDIE and PDIE at the scan rates 1 mV/s.....	49
Figure 4.6 Charge/discharge curves of (a) PDIE (c) NDIE (e) PNDIE and cycling performance of (b) PDIE (d) NDIE (f) PNDIE. Cutoff voltages for (a) -0.8 – 0.4 V; (c) -0.8 – 0.4 V; (e) -0.85 – 0.45 V.	50
Figure 4.7 Charge/discharge curves of (a) NDIE & PDIE (b) NDIE & PNDIE	51

Figure 4.8 (a)/(c) Charge/discharge curves of NDIE coin cell (b)/(d) Corresponding cycling performance and coulombic efficiency curves ((a)/(b) without CP (c)/(d) with regular CP (e)/(f) with large CP)	52
Figure 4.9 Schematic diagram of new designed coin cell for NDIE	53
Figure 4.10 A comparison of cycling performance of NDIE coin cells	53
Figure 4.11 (a) Charge/discharge curves of PNDIE ^{1st(1-8)} coin cell (a') Corresponding cycling performance and coulombic efficiency curves	54
Figure 4.12 (a) Charge/discharge curves of PNDIE ^{2nd} coin cell (a') Corresponding cycling performance and coulombic efficiency curves	54
Figure 4.13 (a)/(c) Charge/discharge curves of PDIE coin cell (b)/(d) Corresponding cycling performance and coulombic efficiency curves ((a)/(b) without CP (c)/(d) with CP)	55

List of Tables

Table 1.1 History of battery	4
Table 1.2 Common commercial battery systems.....	4
Table 1.3 Organic carbonates and esters as electrolyte solvent.....	12
Table 2.1 Some inorganic electrode materials	18
Table 3.1 General description of the four imide-based samples.....	30
Table 3.2 Some equipment used during experiments	30
Table 4.1 Characteristic IR band assignments of the four samples	46

Chapter 1 Introduction

The world we are living in needs energy. The major energy we use today can be summarized as oil, coal, peat, shale, natural gas, biofuels and waste, and electricity. However, the energy we cannot live without has been consumed too fast. The climate changes along with too much CO₂ emissions also draw lots of attention. Everybody knows that energy is central to achieving the interrelated economic, social, and environmental aims of sustainable human development. It is never too late for us to realize that both the kinds of energy we produce and the ways we use them need to change. According to the Jose Goldemberg, chair of World Energy Assessment, energy systems that lead to a more equitable, environmentally sound, and economically viable world will be created [1].

That is why electrochemical energy conversion and storage systems, including batteries, fuel cells, and supercapacitors are definitely playing an important role as an alternative because the energy consumption is designed to be more sustainable and more environmentally friendly. Among all these choices, batteries, especially rechargeable lithium-ion batteries (LIBs), can be treated as such an interesting and worthy topic to investigate in so many labs all over the world. A battery contains one or more electrically connected electrochemical cells having terminals/contacts to supply electrical energy. The rechargeable lithium-ion battery is one of the most promising candidates since it has so many advantages compared to others, such as its higher energy density (up to 180Wh/kg), higher cell voltage (up to about 3.8 V per cell), and longer shelf life (up to 5 – 10 years). And its market has grown in decades from a research & development interest to sales of over 1.1 billion units with value of over \$4 billion by 2005 [2].

1.1 Batteries and Other Energy Storage Devices

Batteries, fuel cells and electrochemical capacitors all belong to devices for electrochemical energy storage and conversion. While there are “electrochemical similarities” among these three systems, the energy storage and conversion mechanisms are different. The similarities are that the energy-providing processes take place at the phase boundary of the electrode/electrolyte interface and the electron and ion transport are separated. However, batteries have found by far have the most application markets and have an established market position [3]. They can be used in portable electronics, cars, electrical vehicles (EVs), toys, renewable energy and electric grid and building storage, etc. In addition to well-known batteries such as lead-acid and lithium-ion batteries, there are many other types of cells in the long river of battery development. A short history will be given in the next section.

1.1.1 Brief History of Batteries

The earliest battery was discovered two thousand years ago (from the Parthian period, roughly 250 ECB to A.D. 250). A clay jar sealed with pitch at its top opening was found from an ancient tomb by workers who were constructing a new railway near the city of Baghdad [4]. Sticking through the seal was an iron rod surrounded by a copper cylinder (see Figure 1.1a). With vinegar or any other electrolytic solution inside, the jar produces about 1.1 volts. The next major battery-related research was conducted in 1786 when Luigi Galvani noticed the reaction of frog legs to voltage, so-called “animal electricity” [5]. He thought the reaction was due to a property of the tissues, which was not the real case.

Later on, in 1800, Alessandro Volta published details of a battery. That battery was made by piling up layers of silver, paper or cloth soaked in salt, and zinc. Thirty-six years later, since the Voltaic Pile was not good for delivering currents for long periods of time, the Daniell Cell was developed by British researcher John Frederick Daniell. The first Daniell cell was made of a hollow bullhorn, which was replaced by porous vases later, filled with diluted sulfuric acid in which a cylindrical stem of zinc (as anode) was immersed. A copper cylinder (as cathode) filled with a saturated copper sulfate solution surrounded this system (see Figure 1.1b) [6, 7].

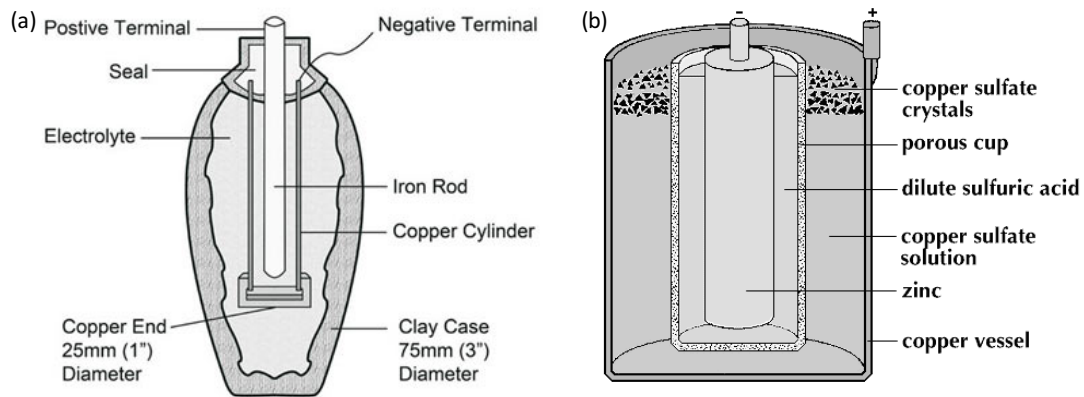


Figure 1.1 Structure of (a) a Baghdad battery and (b) a Daniell cell

Then, in 1859, the first rechargeable battery, a lead-acid battery, was invented by French physicist Gaston Planté. It has been widely used in the car. However, it has quite low energy density and only 500-1500 cycles can be maintained due to material mechanical stress. Also, it does not like deep cycling because a full discharge causes extra stress and each cycle robs the battery of some service life. Furthermore, it is essential to have a fully saturated charge periodically; this can help avoid sulfation and keep the battery stored in a charged state. All of these problems are forcing people to constantly look for a better and safer battery for their cars. More history of battery

development can be found in the Table 1.1 and some common commercial battery system can be found in the Table 1.2.

Table 1.1 History of battery

Year	Inventor	Discovery and Invention
250 ECB - 250 AD	Unknown	Baghdad Battery
1786	Luigi Galvani	Animal Electricity
1800	Alessandro Volta	Voltaic Pile
1836	John Frederick Daniell	Daniell Cell
1859	Raymond Gaston Planté	Lead Acid
1866	Georges Leclanché	Carbon-Zn Dry Cell
1910	Thomas Edison	Zn/Ni and Fe/Ni Cells
1893 – 1909	Jungner and Berg	Nickel-Cadmium Battery
1949	Lew Urry	Alkaline-Manganese Battery
1950	Samuel Ruben	Zn/HgO Alkaline Battery [8]
1964	Procter & Gamble	Duracell is formed (incorporated)

Table 1.2 Common commercial battery systems [3]

common name	nominal voltage	anode	cathode	electrolyte
primary				
Leclanché (carbon–zinc)	1.5	zinc foil	MnO ₂ (natural)	aq ZnCl ₂ –NH ₄ Cl
zinc chloride (carbon–zinc)	1.5	zinc foil	electrolytic MnO ₂	aq ZnCl ₂
alkaline	1.5	zinc powder	electrolytic MnO ₂	aq KOH
zinc–air	1.2	zinc powder	carbon (air)	aq KOH
silver–zinc	1.6	zinc powder	Ag ₂ O	aq KOH
lithium–manganese dioxide	3.0	lithium foil	treated MnO ₂	LiCF ₃ SO ₃ or LiClO ₄ ^a
lithium–carbon monofluoride	3.0	lithium foil	CFx	LiCF ₃ SO ₃ or LiClO ₄ ^a
lithium–iron sulfide	1.6	lithium foil	FeS ₂	LiCF ₃ SO ₃ and/or LiClO ₄ ^a
rechargeable				
lead acid	2.0	lead	PbO ₂	aq H ₂ SO ₄
nickel–cadmium	1.2	cadmium	NiOOH	aq KOH
nickel–metal hydride	1.2	MH	NiOOH	aq KOH
lithium ion	4.0	Li(C)	LiCoO ₂	LiPF ₆ in nonaqueous solvents ^a
specialty				
nickel–hydrogen	1.2	H ₂ (Pt)	NiOOH	aq KOH
lithium–iodine	2.7	Li	I ₂	LiI
lithium–silver–vanadium oxide	3.2	Li	Ag ₂ V ₄ O ₁₁	LiAsF ₆ ^a
lithium–sulfur dioxide	2.8	Li	SO ₂ (C)	SO ₂ –LiBr
lithium–thionyl chloride	3.6	Li	SOCl ₂ (C)	SOCl ₂ –LiAlCl ₄
lithium–iron sulfide (thermal)	1.6	Li	FeS ₂	LiCl–LiBr–LiF
magnesium–silver chloride	1.6	Mg	AgCl	seawater

^a In nonaqueous solvents. Exact composition depends on the manufacturer, usually propylene carbonate–dimethyl ether for primary lithium batteries and ethylene carbonate with linear organic carbonates such as dimethyl carbonate, diethyl carbonate, and ethylmethyl carbonate for lithium ion cells.

1.2 Lithium-ion Batteries

Lithium is the most electropositive element (high voltage); lithium is the lightest metallic element with atomic weight 6.94 atomic mass unit (high specific energy); lithium ions are small for fast diffusion (high power). All these advantages make lithium a great candidate for electrode materials. As a result, serious development of high-energy-density batteries was started in the 1960s and concentrated on non-aqueous primary batteries using lithium as the anode and it was also used in selected military applications in the early 1970s [2]. However, using lithium itself as an anode exhibits a serious defect; its dendrite formation will directly lead to its failure as an anode. Moreover, this safety issue and other problems still exist as challenges right now, such as the limitation as suitable cell structures, formulations and so on.

All these difficulties urged researchers looking for a way to avoid the drastic morphological change of the anode during cell cycling. Consequently, the “rocking chair” concept and other intercalation-type electrodes have been put forward [9-12]. According to Whittingham, Goodenough et al., most of the host materials are transition metal oxides or chalcogenides with stable crystal lattices. Therefore, their layer or tunnel structures can provide a route for guest ions such as the lithium ion to diffuse. About exactly how the transition metal oxides as an anode work, a more detailed mechanism can be found in Section 1.2.1.

From lithium to lithium-ion, from primary battery to rechargeable battery, so many hard works and efforts have been paid. But the sweats were not in vain, since lithium-ion battery was developed, it has occupied a significant position as energy storage devices in lots of applications, ranging from portable electronics to electric vehicles. However, the

general demands for lighter, thinner, and higher capacity lithium ion batteries require ongoing research for novel materials with improved properties over that of state of the art. Such an effort necessitates a concerted development of both electrodes and electrolyte to improve battery capacity, cycle life, and charge-discharge rates while maintaining the highest degree of safety available [13, 14].

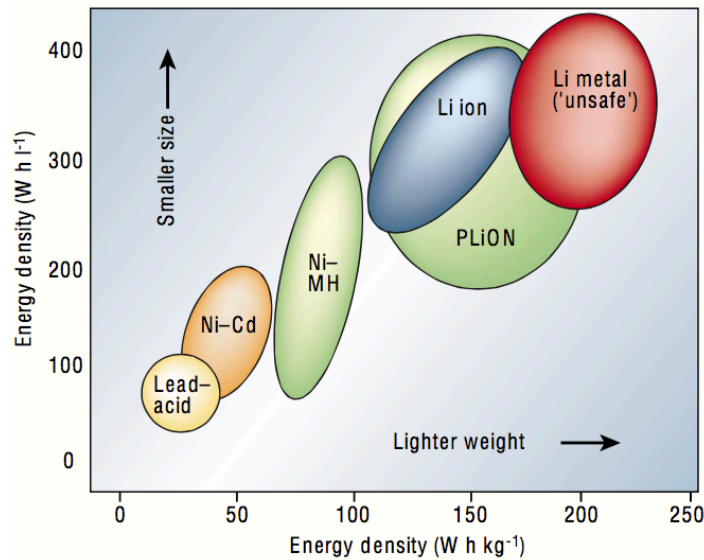


Figure 1.2 Comparison between different rechargeable battery technologies in terms of volumetric and gravimetric energy densities [15]

Figure 1.2 emphasizes the relationship of some predominant rechargeable batteries between specific and volumetric energy density. The general purpose for battery development is to increase energy and power densities, while minimizing volumetric and mass limitations (i.e., move to the upper right of Figure 1.2). Portable electronics (e.g., cellular phones, PDAs, laptops, etc.) are terrific examples where consumer demand imposes both smaller and lighter batteries that require minimal time to charge, but without compromising talk time or usable battery life. Such a balance between energy density and rate has driven lithium ion technology to the forefront. Therefore, in response to these expectations, the next generation of lithium ion batteries will need to achieve

higher specific capacities, faster C-rates (time for cell discharge in reciprocal hours), increased safety, and appropriate cyclability [14-16].

1.2.1 Basic Principles of Lithium-ion Battery

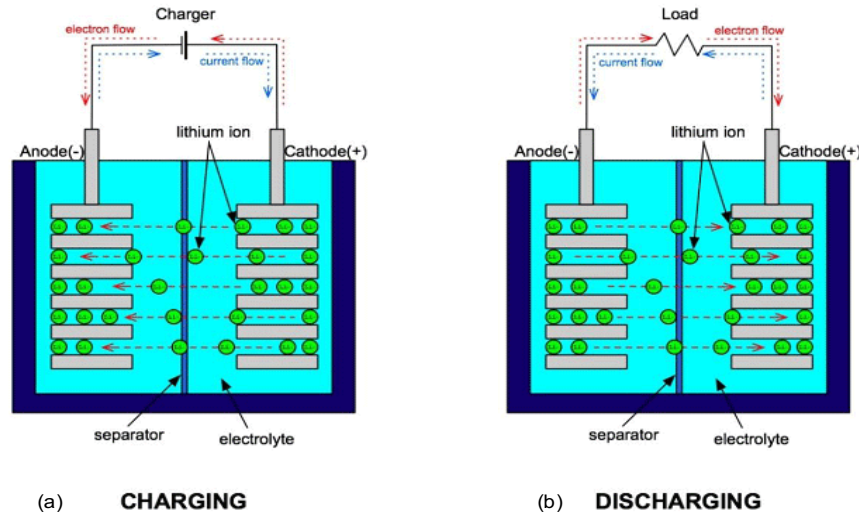


Figure 1.3 The lithium-ion battery mechanism

Typically, a lithium ion battery operates by shuttling lithium ions from the cathode to the anode upon charging and the reversible process occurs during discharge, as shown in Figure 1.3. The lithiated metal oxides and graphitic carbons are layered materials with interstitial spaces receptive to lithium ion intercalation. The active material is able to store the lithium due to the simultaneous electron transport from the current collector to reduce the lithium ion at the active material “host” site. The intercalation process is aided by a necessary solid-electrolyte-interface (SEI) that forms on the surface of each electrode, which serves a critical role, namely, to passivate the electrode surface from further solvent reduction and to act as a selective layer to allow only lithium ions to diffuse. It is very dangerous if the SEI is not uniform or is broken. More details will be given in the challenge section.

1.2.2 Typical Electrode Material

Different electrode materials for rechargeable Li-based cells are shown below in Figure 1.4. For the anode part, the lower the potential the better and for the cathode part, the higher the better.

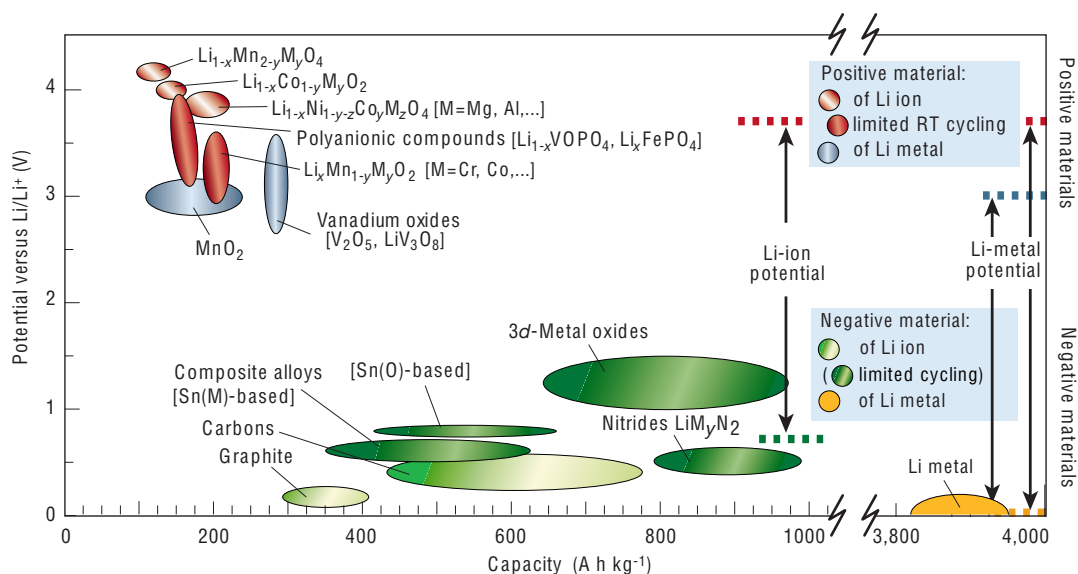


Figure 1.4 Voltage versus capacity for positive and negative electrode materials [15]

1.2.2.1 Traditional Anode Electrode Materials

The most fundamental anode material for lithium-based batteries is definitely metallic lithium, which has been used in primary batteries from almost sixty-years ago. For secondary lithium-based batteries, however, the drawback leads to danger. Therefore, carbonaceous materials were shown up as very good candidates due to low cost, low Li-ion insertion potential ($\sim 0.1\text{V}$ vs. Li/Li^+), and good cycling stability. Most importantly, using carbon materials as a lithium reservoir at the negative electrode could prevent dendrite formation during lithium repeat insertion into the carbon host.

Among carbon materials, graphite is a commonly used anode material in rechargeable lithium batteries due to its high coulombic efficiency [17]. However, the

specific capacity of graphite is relatively low. Therefore, many other carbon materials have been studied, such as natural and synthetic graphites, graphitizable carbons, low-temperature and non-graphitizing carbons and doped carbons [18]. As shown on the left side of Figure 1.5, soft carbon, hard carbon and graphite are three major types of carbon used in lithium-ion batteries [19]. The first commercialized rechargeable LIB, sold by Sony in 1991, used soft carbon as an anode. Soft carbon was replaced by hard carbon (i.e., non-graphitizable carbon) because of its enhanced specific capacities [20]. From Figure 1.5 we can see their typical potential performance.

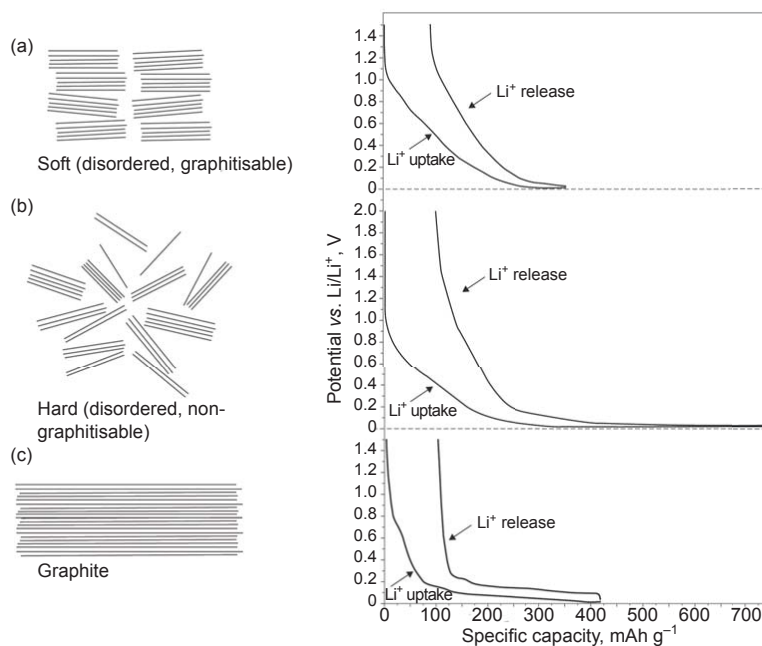


Figure 1.5 (Left side) The structures of (a) Soft carbon (b) Hard carbon and (c) Graphite; (Right side) Their typical potential performances [20]

Except carbonaceous materials, another good candidates for anode are lithium-metal alloys. They are good because they have a relatively high-energy capacity and safety characteristics. Their reactions with lithium have been widely studied since the 1970s. The shortcomings of alloy anodes are low cycle life and high initial capacity loss [21]. This is because the large volume expansion/contraction upon lithiation and

delithiation leads to a cracking and pulverization of active material particles and therefore loss of electronic contact from the conductive carbon or current collector [22, 23].

Transition metal oxides have always been used as cathode materials until they were demonstrated as a good anodes because lithium-ions could intercalate and deintercalate into/from their structure reversibly [24]. Generally, transition metal oxides have two different mechanisms of intercalation and de-intercalation. The basic difference is during the process, one mechanism will accompany the formation of Li_2O and the other will not.

1.2.2.2 Conventional Cathode Electrode Materials

Host material must satisfy the following needs: It must be stable upon lithium insertion/extraction, have high potential, be electronically and ionically conducting, and be stable with the electrode. Generally, lithium-based metal oxides have been used as cathode materials. At present, almost all cathode materials research has been focused on LiMO_2 ($\text{M}=\text{Co}$, Ni , Mn and so on), LiMn_2O_4 , and LiMPO_4 ($\text{M}=\text{Fe}$, Mn , V and so on).

The LiMO_2 compound has a two-dimensional layered structure (see Figure 1.6). It typically contains layered compounds with an anion close-packed or almost close-packed lattice in which alternate layers between the anion sheets are occupied by a redox-active transition metal. Lithium then inserts itself into the essentially empty remaining layers [25]. Take LiCoO_2 as an example: it has a high voltage, high capacity, good mixed conductor, and moderately long cycle life. However, the LiCoO_2 is unsafe when overcharged, and it is toxic and expensive.

LiMn_2O_4 has a three-dimensional spinal structure (see Figure 1.6). This material has the following advantages: Mn is cheap, environmentally benign, safe, and has high

rate capability. But the performance of LiMn_2O_4 is very poor due to Mn dissolution in electrolyte, consistent generation of H_2O , and Jahn-Teller distortion.

LiMPO_4 has an olivine structure (see Figure 1.6). Take LiFePO_4 as an example; this compound has similar advantages with the previous one. The problem is that LiFePO_4 has poor conductivity, so the material needs to go nano size and have a surface coating.

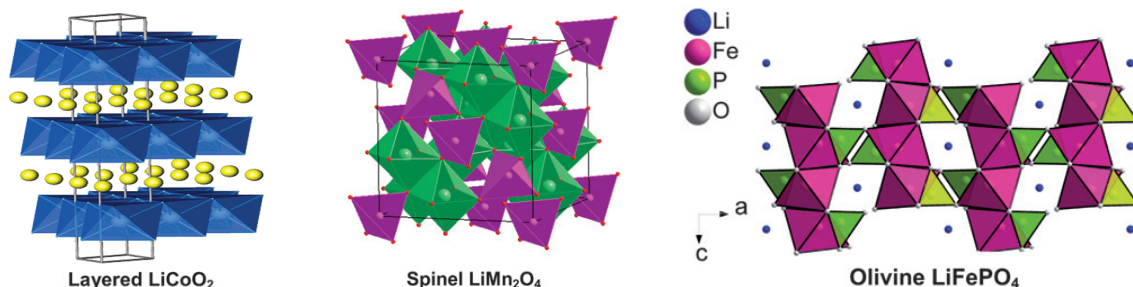


Figure 1.6 Crystal structures of conventional cathode materials for lithium-ion batteries [25, 26]

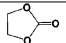
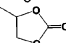
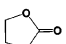
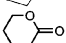
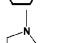
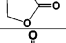
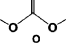
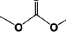
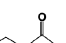
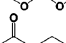
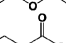
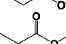
1.2.3 Non-aqueous Liquid Electrolyte

Typically, a cell must consist of a positive and a negative electrode separated by an electrolyte. Electrolytes are ubiquitous and indispensable in all electrochemical devices, serving as the medium for the transfer of ions, between a pair of electrodes. It seems like the electrolyte is in very close position with both electrodes. So, the need for seeking compatible electrolytes always arises with the appearance of new electrode materials. Back in the 1950s, the lithium metal was found to be stable in lots of non-aqueous solvents due to the SEI layer we mentioned in Section 1.2.1 [27]. Later on, in the 1960s and 1970s, the range of electrolyte solvents extended from organic (propylene carbonate) to inorganic (thionyl chloride and sulfur dioxide) [28-30].

Most electrolytes for lithium-ion batteries contain one or more (usually one) lithium salts in mixtures of two or more solvents. Different solvents are used together to

achieve the performance that can satisfy various functions simultaneously. Some common solvents are given in the Table 1.3 below.

Table 1.3 Organic carbonates and esters as electrolyte solvent [27]

Solvent	Structure	M. Wt	T _m / °C	T _b / °C	η/cP 25 °C	ε 25 °C	Dipole Moment/debye	T _f / °C	d/gcm ⁻³ , 25 °C
EC		88	36.4	248	1.90, (40 °C)	89.78	4.61	160	1.321
PC		102	-48.8	242	2.53	64.92	4.81	132	1.200
BC		116	-53	240	3.2	53			
γBL		86	-43.5	204	1.73	39	4.23	97	1.199
γVL		100	-31	208	2.0	34	4.29	81	1.057
NMO		101	15	270	2.5	78	4.52	110	1.17
DMC		90	4.6	91	0.59 (20 °C)	3.107	0.76	18	1.063
DEC		118	-74.3 ^a	126	0.75	2.805	0.96	31	0.969
EMC		104	-53	110	0.65	2.958	0.89		1.006
EA		88	-84	77	0.45	6.02		-3	0.902
MB		102	-84	102	0.6			11	0.898
EB		116	-93	120	0.71			19	0.878

1.3 Different Forms of Lithium-ion Batteries

One or more electrochemical units (“cells”) constitute a battery. According to the way cells are connected, the configurations of a battery can be grouped as: cylindrical, coin, prismatic, thin and flat (as shown in Figure 1.7). These various connected methods, in series or parallel or both, depend on the desired output voltage and capacity. Besides the anode, cathode and electrolyte, another important constituent in a cell is a separator. There are two functions that a separator has. First, a separator can keep two electrodes apart. Second, a separator functions like a breaker. When temperature inside a cell goes too high, a separator would melt, thereby leading to a short circuit and maintaining a safe environment. In my experiments, the coin cell has been chosen as the configuration to test the performance of anode electrode materials.

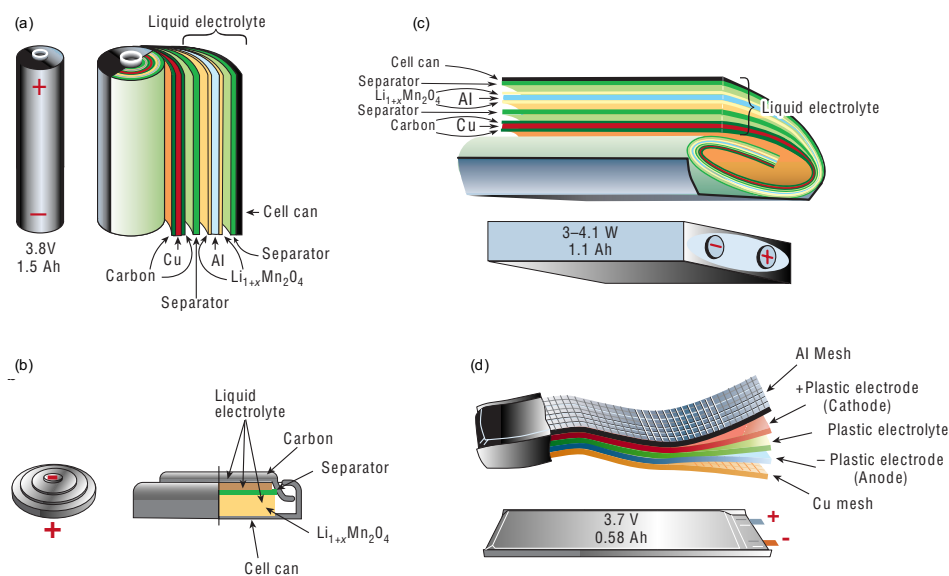


Figure 1.7 Various lithium-ion battery configurations (a) Cylindrical (b) Coin (c) Prismatic and (d) Thin and flat [15]

1.4 Safety Issue in Non-aqueous Rechargeable Lithium Batteries

The main issues in organic rechargeable lithium batteries include high cost, insufficient cycle life, and poor safety characteristics. Among these barriers, safety is always the most important issue, which requires further development of a nonflammable electrolyte. Major challenges are related with the thermal stability of anodes or cathodes, as well as separators and electrolytes inside the battery when temperature goes too high. Both the thermal instability and occurrence of internal short circuits would lead to thermal runaway, i.e., fires or explosions.

In an ideal case, when lithium ions are shuttled between two electrodes, almost all the lithium ions can be inserted/removed from the corresponding electrode reversibly. The coulombic efficiency can reach 100% and there are no side reactions. However, in a real case, the efficiency is a little bit lower than 100% and several surface side reactions occur during the charging and discharging process. For example, a highly oxidative transition-metal oxide is formed at the positive side and highly reductive lithiated

graphite is generated at the negative side [31]. There are bad influences on the cell performance when side reactions happen. First of all, the capacity may decrease since the side reactions consume nearby lithium or other active electrode materials. This capacity decrease may also happen when some by-products deposit on the surface of active electrode material and therefore block the way for charge transfer. Moreover, these side reactions can be kinetically accelerated and release large amounts of heat at elevated temperature or under abuse environments in a very short period of time. These phenomena are very dangerous and could lead to fire or explosion.

1.5 Background of Aqueous Rechargeable Lithium-ion Battery

The aqueous rechargeable lithium-ion battery (ARLB) is an emerging battery technology first raised in the mid-1990s. At that time, ARLB as a new type of rechargeable lithium-ion battery with an aqueous electrolyte was reported [32, 33]. This battery uses lithium-intercalation compounds such as LiMn_2O_4 , $\text{LiNi}_{0.81}\text{Co}_{0.19}\text{O}_2$, and VO_2 as the electrode material and an alkaline or neutral aqueous electrolyte [32-34]. By using aqueous electrolytes, the cells can overcome the disadvantages of non-aqueous ones, such as high cost, safety problems, and environmental pollution problems [35]. In addition, higher concentration of salts (2.5 mol/L Li_2SO_4) and lower viscosity of water dramatically improve the ionic conductivity and mobility in an aqueous electrolyte system. Hence, higher C-rate performance can be expected [36].

Aqueous lithium-ion batteries that combine the “rocking-chair” principle of conventional LIBs and the use of low cost, nonflammable aqueous electrolyte offer a significant advantage over the ones that use organic electrolyte in terms of safety, flexibility in vehicle design, and system cost reduction.

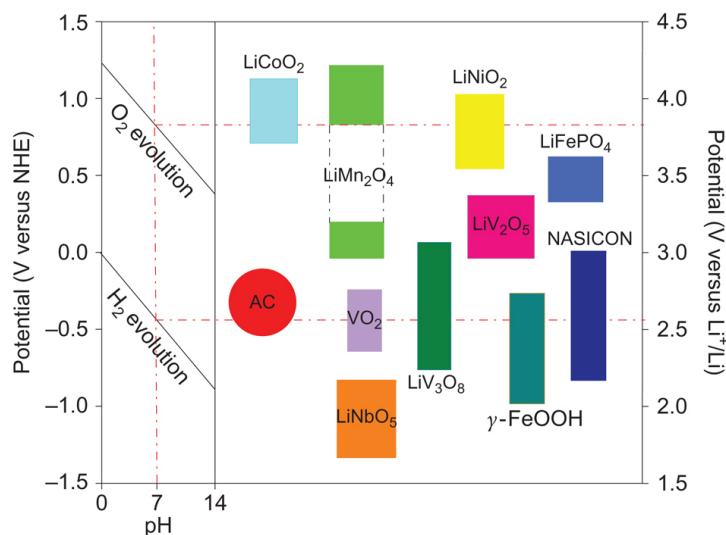


Figure 1.8 (Left side) O₂/H₂ evolution potential vs. NHE for different pH; (Right side) Intercalation potential of various lithium-ion electrode materials vs. NHE and Li/Li⁺ [37]

Despite the many advantages of aqueous electrolytes, water has a low thermodynamic stability window (1.23 V), resulting in a lower energy density than current Li-ion batteries. The position of water's stability window shifts with pH, specifically at 0.059 V per pH unit, as can be seen from the Pourbaix diagram (left side of Figure 1.8). The right part of Figure 1.8 shows the intercalation potential of some electrode materials that could possibly be used in aqueous Li-ion batteries. In reality, many aqueous batteries can function well above the thermodynamic limits. For example, the voltage of a Pb-acid battery can reach up to 2.0 V due to the high hydrogen overpotential of Pb as well as electronically insulating but ionically conductive PbSO₄, across which there is a steep potential gradient [38]. Nevertheless, the chemical/electrochemical processes of lithium-ion intercalated electrode materials in aqueous solutions are much more complicated than those in the organic electrolytes.

1.6 Challenges in Aqueous Lithium-ion Batteries

So far, we have discussed advantages, i.e., high ionic conductivities, low cost, and increased safety; and disadvantages, i.e., narrow stability window and poor cycling, of ALIBs in general. Here, I want to summarize the main challenges of ALIBs and give more detailed explanation. During the charge and discharge process, different kinds of side reactions are involved, which turn out to be the culprit and cause a reduced reversibility of the cells. According to a chemical review about aqueous rechargeable lithium ion batteries, the major challenges – side reactions – are focused on reactions between electrode materials and H_2O or residual O_2 in an aqueous electrolyte, H_2 and O_2 evolution from electrolyte decomposition, electrode dissolution in an aqueous electrolyte, and proton co-insertion with guest ions [39].

The chemical stability of the electrode materials in H_2O is very important. Side reactions between Li and H_2O are detrimental to the cycle stability. When the redox voltage is lower than $V(x)$, the voltage of lithium-ion intercalated compounds (LICs), undesirable reactions can occur in electrode materials. The majority of cathode electrodes are stable against this reaction because their redox potentials are generally higher than $V(x)$ [37]. However, that is not the case with the anode side. The chemical stability of the anode is more vulnerable since the redox potentials of anodes are typically located near $V(x)$ [39]. Even worse, the presence of oxygen leads to the further decrease of electrode materials. Taken together, precise control of the cutoff voltage at a certain pH and elimination of residual O_2 in the electrolyte are very necessary for a stable performance of aqueous cells.

The evolution of hydrogen and oxygen is another important factor people should pay attention to when designing a long-term cycle life battery. Beyond the narrow window (about 1.23V), aqueous electrolytes are prone to decompose and generate H₂ and O₂. Even though sometimes the stability limit can be expanded to about 2V, side reactions derived from the electrolysis may inevitably occur during long-term cycling. That is why it is that important to control the operating potential of both cathodes and anodes in aqueous rechargeable batteries. Also, since the catalytic effect of the active electrode material itself may lead to water electrolysis, it is better to use a non-catalytic electrode in ALIB systems.

The third and fourth factor may limit long-term cyclability should be electrode dissolution and co-insertion of protons with guest ions into the host electrode. The dissolution of cathodes at a specific pH has often been noticed in previous work [40, 41]. And the co-insertion phenomenon is commonly observed in layered structure materials. According to some literatures, this co-insertion can be reduced by increasing the pH [37]. However, using acidic aqueous electrolytes, i.e. pH less than or equal to 7, can reduce the dissolution of the electrode. Thus, using neutral aqueous electrolytes (pH=7) would be the best solution to reduce the chance of both dissolution and proton co-insertion.

In the past two decades, research on aqueous lithium-ion battery never stopped. People have done a lot of work, hoping to solve or avoid the above problems and get a battery that have higher capacity and longer cycle life. Some literatures, involved both inorganic and organic electrode materials, will be reviewed in next chapter.

Chapter 2 Literature Review

2.1 A Brief Review of Inorganic Electrode Materials in ARLBs

Compared with organic electrode materials, the research towards inorganic materials started much earlier. Some inorganic electrode materials, which have been studied the most often, will be given in the Table 2.1 [42].

Table 2.1 Some inorganic electrode materials

No.		Potentials of redox peaks	Aqueous electrolytes
Cathode materials			
1	LiCoO ₂	0.708/0.628V (vs. SCE)	0.5 M Li ₂ SO ₄
2	LiMn ₂ O ₄	0.78/0.73 V, 0.92/0.85 V (vs. SCE)	0.5 M Li ₂ SO ₄
3	LiFePO ₄	0.495/−0.270 V (vs. SCE)	0.5 M Li ₂ SO ₄
4	Li[Ni _{1/3} Co _{1/3} Mn _{1/3}] ₂ O ₂	0.68/0.48 V (vs. SCE)	2 M Li ₂ SO ₄
5	LiNiO ₂	0.76/0.2 V (vs. Ag/AgCl)	0.02 M LiOH
6	LiNiPO ₄	0.094/−0.231 V (vs. Hg/HgO)	LiOH
7	LiMnPO ₄	0.02/−0.3 V (vs. Hg/HgO)	LiOH
Anode materials			
1	VO ₂ (B) nanorods	−0.278/−0.063/−0.341 V (vs. Ag/AgCl)	2.5 M LiNO ₃
	VO ₂ (B) nanoflakes	0.06/−0.32 V (vs. Ag/AgCl)	2.5 M LiNO ₃
	VO ₂ (B) nanoflowers	−0.314/−0.045 V, −0.786/−0.465 V (vs. Ag/AgCl)	2.5 M LiNO ₃
2	V ₂ O ₅ ·nH ₂ O	0.03/0.25 V, 0.71/0.55 V (vs. SCE)	Saturated LiNO ₃
3	H ₂ V ₃ O ₈	−0.43/−0.61 V (vs. SCE)	5 M LiNO ₃
4	MoO ₃	−0.39/−0.32 V, −0.75/−0.59 V (vs. SCE)	0.5 M Li ₂ SO ₄
5	LiV ₃ O ₈	0.1/−0.35 V (vs. NHE)	1 M Li ₂ SO ₄ or LiCl
6	LiTi ₂ (PO ₄) ₃	−0.52 V/−0.36 V (vs. NHE)	5 M LiNO ₃
7	Li ₂ Mn ₄ O ₉		6 M LiNO ₃

2.1.1 Cathode Materials

The spinel LiMn₂O₄ was first introduced by Thackeray et al. as a cathode material for LIB in 1983 [43-45]. It still is one of the best choices of cathode materials due to its low cost and stable crystal structure. However, severe capacity fading has always been the biggest challenge for this material. Dissolution of Mn²⁺ into the electrolyte and generation of new phases during cycling and the related micro-strains are two main reasons lead to this problem [46]. Q.T. Qu et al. reported the porous LiMn₂O₄, which consists of nano-grains, as a cathode material for ARLBs [47]. This porous LiMn₂O₄ was prepared by using polystyrene as a template for the first time. It shows excellent

electrochemical performance in terms of high rate capability, high power density, and long cycling behavior. The crystalline porous structure allows for favorable electrochemical performance of Li^+ intercalation/deintercalation into/from the LiMn_2O_4 cathode for aqueous rechargeable lithium batteries, which in some degree improve the cycling performance. Figure 2.1a shows the discharge curves of the porous LiMn_2O_4 electrode at different current densities when the current density of charge was at a fixed number (100 mA/g). And Figure 2.1b shows the comparison between the solid one and porous one at 1000 mA/g (use activated carbon as the counter electrode). The capacity retention of porous LiMn_2O_4 after 10000 cycles at 9C with 100% depth of discharge is 93%. The main reason for its excellent electrochemical performance is because it is nano size, has porous morphology, and has high crystalline structure. In addition, the acid-free aqueous electrolyte also prevents Mn^{2+} from dissolution.

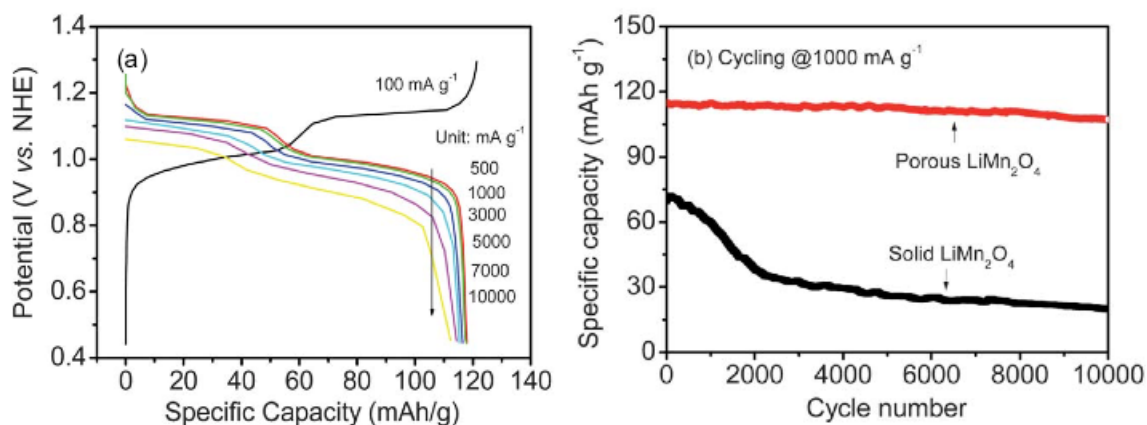


Figure 2.1 (a) The discharge curves of the porous LiMn_2O_4 electrode (b) The cycling behaviors of the solid and porous LiMn_2O_4 electrodes [47]

LiCoO_2 is another cathode material and it is the most widely used in traditional LIBs; its intercalation/deintercalation in aqueous electrolyte is similar to that in the organic one [48]. It has relatively high voltage, high capacity, and long cycle life.

However, the latest data shows that its capacity is about only 120 mAh/g, and it can discharge and charge at 10C with capacity less than 90 mAh/g [49]. Tang's group proposed a nano-LiCoO₂, which was prepared at low temperature (550°C) and for the first time it was used to demonstrate a reversible capacity of 143 mAh/g at 7C and 133 mAh/g at 70C in 0.5 mol/L Li₂SO₄ aqueous electrolyte [50]. From Figure 2.2b we can see its cycling behavior is also very good; there is no obvious fading during the initial 40 cycles. This result indicates that the particle size of active materials is very important. It can improve the electrochemical performance at high current density in aqueous electrolytes.

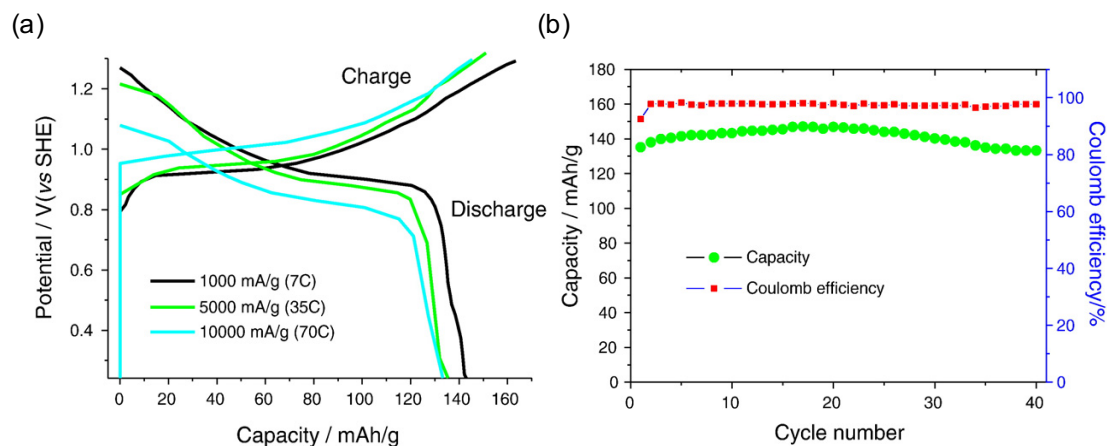


Figure 2.2 (a) Charge/discharge curves at different C-rates (b) Cycling performance at 7C of the as-prepared nano-LiCoO₂ in 0.5 mol/L Li₂SO₄ aqueous electrolytes [50]

G.J. Wang et al. also reported LiCoO₂ as a positive electrode in ARLB [51]. In their report, LiV₃O₈ was chosen as the negative electrode and saturated LiNO₃ solution was chosen as the electrolyte. The result indicates LiCoO₂ has a good cycling stability and can be used as a power source for EVs. Figure 2.3a shows the charge and discharge curves of LiV₃O₈//LiCoO₂, the current density was kept constant at 0.2mA/cm²; and the

capacity was calculated based on the weight of the positive electrode. Figure 2.3a shows the voltage profiles in organic electrolytes and aqueous electrolytes are similar. Although the capacity of the aqueous one is lower than the organic one, it still proves the truth that this charge/discharge behavior can be transferred into an aqueous solution with the appropriate intercalation/deintercalation voltages. Figure 2.3b shows a cycling performance, with about 65% retention after 40 cycles and about 36% retention after 100 cycles. However, it is already a good result back in 2007.

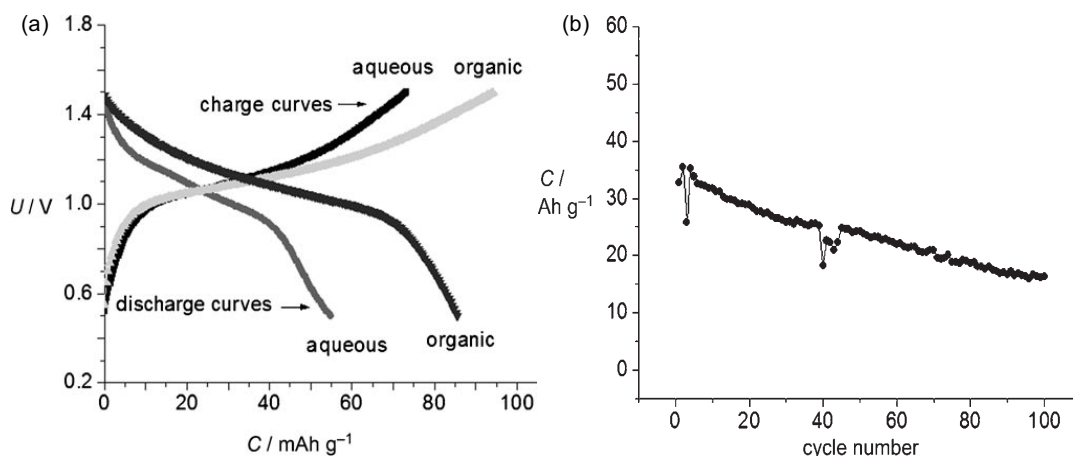


Figure 2.3 (a) Charge/discharge curves for the first cycle of $\text{LiV}_3\text{O}_8//\text{LiCoO}_2$ cells in organic and aqueous electrolytes (b) Cycling behavior of $\text{LiV}_3\text{O}_8//\text{LiCoO}_2$ in aqueous electrolytes at 1 C [51]

2.1.2 Anode Materials

Cathode materials commonly used in non-aqueous LIBs are generally stable in aqueous electrolytes. The challenge is at the anode side; the current inorganic anodes show relative low capacity, are expensive due to costly transition metal being used, and show poor cyclability due to materials dissolution in electrolyte.

H.B. Wang et al. reported an improvement of cycling performance of a lithium-ion cell by coating polypyrrole on the anode side [52]. This lithium-ion cell, $\text{LiMn}_2\text{O}_4//5\text{M LiNO}_3/\text{Li}_x\text{V}_2\text{O}_5$, was assembled in their study. According to their study, the main reasons

of capacity fading of this cell may be attributed to the crystalline structure and phase transformation of $\text{Li}_x\text{V}_2\text{O}_5$, and the dissolving of the V-ion during cycling process. It means the anode side has more effect on cycling performance. In order to stabilize the cycling life, polymerization of pyrrole on the surface of $\text{Li}_x\text{V}_2\text{O}_5$ particles was implemented. There is an obvious improvement in the electrochemical performance after coating PPy on the anode side. In Figure 2.4a/c we can see the difference is very obvious. Figure 2.4c shows that with a coated anode, 86% capacity retention was achieved after 40 cycles and 82% after 60 cycles. However, only 8% of the original capacity remains after 40 cycles for the cell with a bared anode. In addition, as you can see in Figure 2.4b the cell with coated anode also delivers a specific capacity of 43 mAh/g at an average voltage of 1.15 V. Figure 2.4b shows the second cycle of the charge/discharge curve and was conducted in 5M LiNO_3 aqueous electrolyte. This study demonstrates that surface coating with a conductive polymer can effectively improve the cycling stability of a lithium-ion battery with aqueous electrolyte.

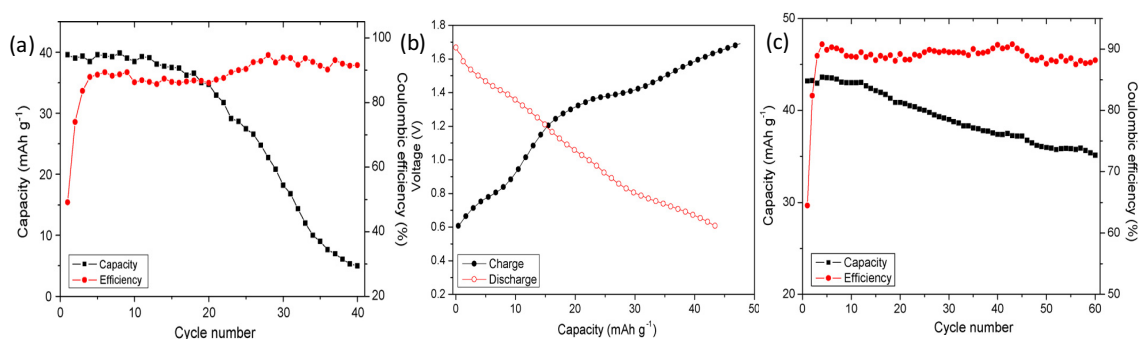


Figure 2.4 (a) Cycling performance and coulombic efficiency curves of cell before coating PPy on bare anode (b) Charge/discharge curves of $\text{LiMn}_2\text{O}_4/\text{Li}_x\text{V}_2\text{O}_5\text{-PPy}$ cell (c) Cycling performance and coulombic efficiency curves of cell after coating PPy [52]

NASICON-structure $\text{LiTi}_2(\text{PO}_4)_3$ has high capacity, suitable potential, and a flat voltage plateau in aqueous electrolyte. However, this material has very low electronic

conductivity. Porous, highly crystalline NASICON-phase $\text{LiTi}_2(\text{PO}_4)_3$ was reported by J.Y. Luo and Y.Y. Xia [53]. The material was prepared by a novel poly(vinyl alcohol)-assisted sol-gel route and coated by a uniform and continuous nanometers-thick carbon thin film using chemical vapor deposition technology. The as-prepared $\text{LiTi}_2(\text{PO}_4)_3$ exhibits excellent electrochemical performance both in organic and aqueous electrolytes, and especially shows good cycling stability in aqueous electrolytes (Figure 2.5a). An aqueous lithium-ion battery consists of a combination of LiMn_2O_4 cathode, $\text{LiTi}_2(\text{PO}_4)_3$ anode, and a 1M Li_2SO_4 electrolyte. The cell has a capacity of 40 mAh/g and a specific energy of 60 Wh/kg with an output voltage of 1.5 V based on the total weight of the active electrode materials. It also exhibits an excellent cycling stability with a capacity retention of 82% over 200 charge/discharge cycles.

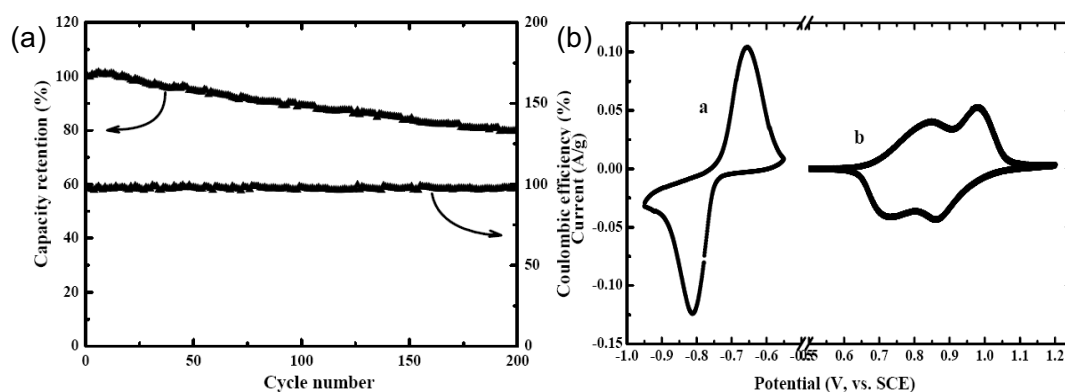


Figure 2.5 (a) Cycling performance of the $\text{LiTi}_2(\text{PO}_4)_3//\text{LiMn}_2\text{O}_4$ aqueous lithium-ion battery at a current rate of 10 mA/cm² (b) CV curves of a $\text{LiTi}_2(\text{PO}_4)_3$ and LiMn_2O_4 at a sweep rate of 0.3 mV/s in 1 M Li_2SO_4 solution [53]

2.2 A Brief Review of Organic Electrode Materials in ARLBs

Although it seems that the real study regarding organic electrode materials started recently, it is actually not new to use organic materials as the active materials for the battery electrode. As early as the 1960s, dichloroisocyanuric acid was used as a cathode

material in a lithium battery [54]. However, for a long time, polymer electrodes have been buried in oblivion due to their poor performance. Recent exciting progress in organic electrodes has brought polymer electrodes to the attention of the energy storage community [55, 56]. Many polymers have been studied as electrode materials for lithium-ion batteries for a long time, especially in the past thirty years. Among all of the candidates, S-S bonds seem to be the most favored structure due to their high theoretical capacity [57-59]. However, low utilization ratio and poor cyclability make it less attractive. There are other choices that people also have interests in and have been working on recently. Some organic materials will be reviewed in the following two sections.

2.2.1 Cathode Materials

Z.P. Song et al. proposed a novel organic cathode material for rechargeable lithium batteries, poly(anthraquinonyl sulfide) by linking the anthraquinone (AQ) unit with the thioether bond [56]. This strategy helps to retain the good reversibility of AQ and effectively improve its cyclability. The cycling test of PAQS proves its high utilization, high coulombic efficiency, excellent cyclability, and satisfactory rate capability. Figure 2.6 shows discharge capacity and coulombic efficiency vs. cycle number in different conditions. The cut-off voltage is 1.4-3.5 V. For Figure 2.6c, current rate increased from 50 mA/g to 500 mA/g, and 40 cycles were performed at each current rate. From Figure 2.6a/b, we can see that although unavoidable dissolution of the active material still exists, ester electrolyte has a better compatibility with the AQ electrode than the ether one.

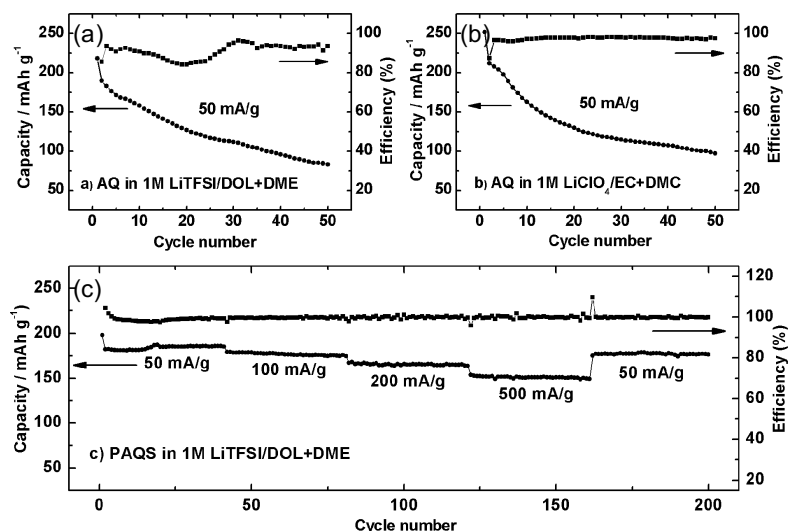


Figure 2.6 Discharge capacity and coulombic efficiency for (a) AQ in 1 M LiTFSI/DOL + DME electrolyte (b) AQ in 1 M LiClO₄/EC + DMC electrolyte (c) PAQS in 1 M LiTFSI/DOL + DME electrolyte [56]

2.2.2 Anode Materials

W.S. Choi et al. reported the electrochemical behavior for a carbonyl-based polymer, poly(2-vinylanthra-quinone) (PVAQ), in aqueous electrolytes [60]. 2-vinylanthraquinone reacted with 1,2-dichloroethane by radical polymerization and yielded PVAQ with a sufficiently high molecular weight. The final polymer electrode became insoluble but swellable and equilibrated in the electrolyte solutions. Spin-coated PVAQ thin film underwent redox reaction in aqueous electrolytes, which allowed the pursuit of the electrochemistry of anthraquinone in H₂O. In Figure 2.7a (white cycle represents charging and black cycle represents discharging), 91% of the initial capacity was maintained even after 300 cycles. The inside figure a' was the charge/discharge result which conducted under 30 wt% NaOH electrolyte (pH=14, 5A/g current density). Also, the charge/discharge curve obtained at 15 °C shows a plateau voltage near 0.75 V/0.5V with the coulombic efficiency of 91%. And the discharge rate were 3, 7, 10, 14, 20, 27, 34 A/g, respectively (Figure 2.7b).

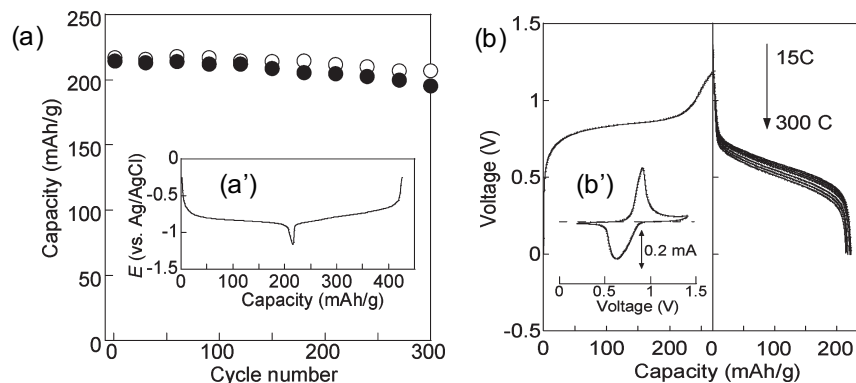


Figure 2.7 (a) Cycle performance of PVAQ (a') Charge/discharge curves of PVAQ (b) Charge/discharge curves of PVAQ/air cell (b') Cyclic voltammogram of the cell [60]

Z.P. Song et al. synthesized a series of imide-based polymers [61]. The dianhydride aromatic imide group can be electrochemically reduced and oxidized in a reversible manner. The voltage profiles and the cycling performance of the polyimides under C/10 are shown in Figure 2.8. Different voltage plateaus were obtained and the specific capacity varies from 160 mAh/g to 200 mAh/g. Both PI-3 and PI-4 have better cycling performance when compared to the other three.

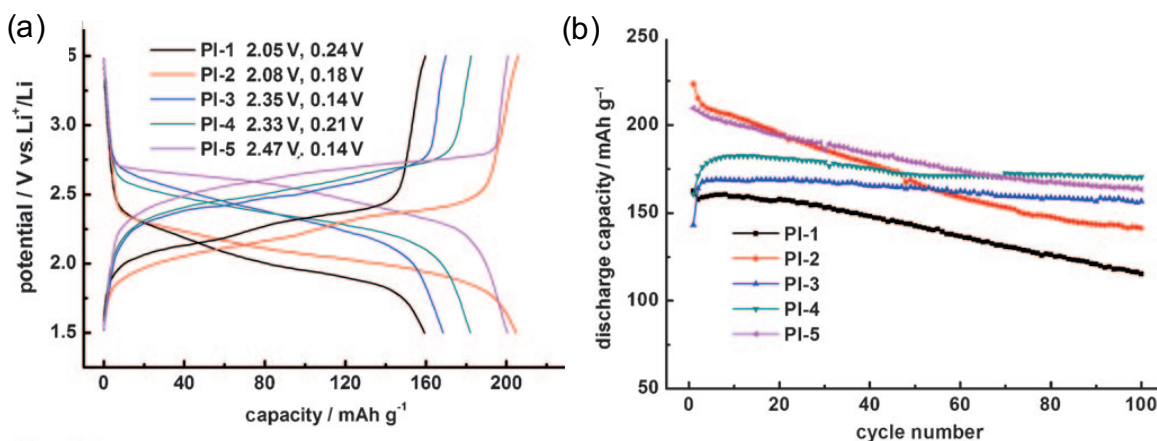


Figure 2.8 (a) Charge/discharge curves for five polyimides under 0.1C (b) Cycle performance for five polyimides [61]

Based on the above performance of polyimides, H. Qin et al. investigated the electrochemical performance of PI-5 in the aqueous system [62]. With polyimide used as

an anode, 5M LiNO₃ as an electrolyte, and LiCoO₂ as a cathode, the cell presents a specific capacity of 71 mAh/g and a specific energy of 80 Wh/kg. This is the best result among all reported ARLBs. It also shows excellent cycling stability and rate capability. Meanwhile, the performance of a polyimide//NaVPO₄F cell in the ARSB system has proved that the polyimide anode has a good capacity performance and cycling stability in 5 M NaNO₃ solution.

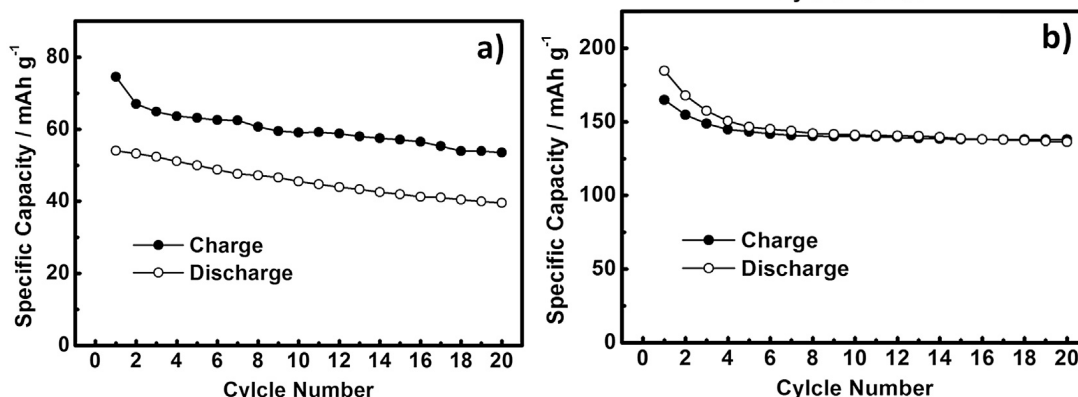


Figure 2.9 Cycling performance of (a) NaVPO₄F and (b) Polyimide in 5 M NaNO₃ solution at a current density of 50 mA/g [62]

In summary, both LiMn₂O₄ and LiCoO₂ in aqueous electrolyte demonstrate good capacity retention and rate capability. For the anode part, although surface coating can somehow suppress inorganic anode dissolution in aqueous electrolyte, good capacity retention still could not be achieved for long cycle life. Also, the capacity of the anode part is not satisfactory. Meanwhile, some organic electrode materials, especially carbonyl-based compounds, have been investigated in organic electrolyte and demonstrated higher capacity and better cycling performance after polymerization. The insoluble property of polymers and their appropriate redox potential make them potential candidates of anode electrode materials in an aqueous system.

Therefore, in my work, we proposed to use organic carbonyl/imide based polymer

anodes coupled with existing lithium transition metal oxide cathodes for application in aqueous lithium ion batteries. For the actual experiments, active carbon was always used as a cathode material, but a similar capacity and cycle life remained when compared with using lithium transition metal. The organic carbonyl compounds (OCCs) were treated as such attractive electrode materials due to their potential sustainability, low cost, and high energy. These properties also were the reason why these compounds were investigated in my research [63, 64]. Carbonyl is a common organic functional group that shows oxidative ability. This process can be reversible with one-electron reduction to form a radical monoanion when it has stabilizing R groups (Figure 2.10) [65]. So it is not a traditional intercalation reaction. Another important functional group discussed below is the imide group. The imide group shows better capacity since it contains two carbonyl groups. The detailed mechanism for imide-based electrode materials will be described in Section 3.1.2.

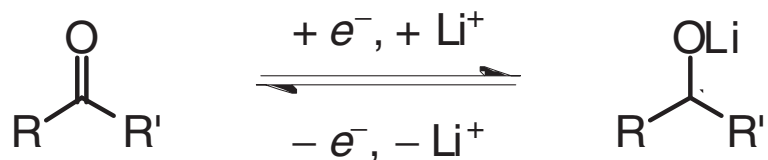


Figure 2.10 Mechanism for reversible reduction of general carbonyl compounds

Chapter 3 Synthesis of Organic Materials

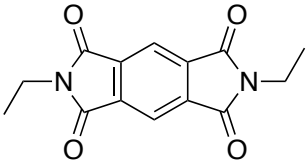
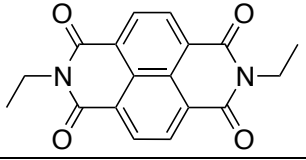
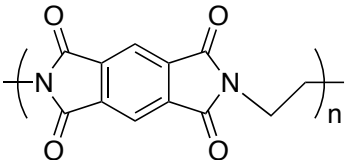
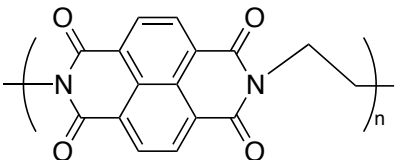
3.1 Materials Design

The objective of this research is to develop suitable anode materials with better performance than conventional inorganic materials. To avoid the unwanted dissolution in the electrolyte and achieve fast kinetic properties, constructing polymer anodes with a stable, inactive framework, and a highly electroactive functional group is key.

Based on the situation just analyzed, we here proposed a group of innovative organic carbonyl monomers and corresponding polymers that not only have high capacities but also are stable in the aqueous electrolyte during cycling. These compounds have such good properties because of several reasons. First, organic carbonyl compounds have very high theoretical capacity. Second, polymers are low cost, and are free from dissolution, which guarantees stable cycling behavior. Third, monomers have relatively small molar mass and no complex synthesis method involved. The last but not the least, reduction potentials can be fine-tuned to maximize cell potentials. From Z.P. Song's work, we already see good performance of PI as a cathode material in organic electrolyte [61]. And comparing with other transition oxide anodes for ARLB, polyimide has more suitable working voltage, higher capacity and better structure stability.

The proposed materials' structures are shown in Table 1. In Table 1, the first two are monomers and the last two are corresponding polymers. PDIE and PPDIE are PMDA-based materials (PMDA = pyromellitic dianhydride) and the NDIE and PNDIE are NTCDA-based materials (NTCDA = 1,4,5,8-naphthalenetetracarboxylic dianhydride).

Table 3.1 General description of the four imide-based samples

Name	Structure	Theoretical capacity (mAh/g)	Redox Potential (V) vs. SHE
PDIE		196.86	-0.577
NDIE		166.28	-0.388
PPDIE		221.35	—
PNDIE		183.40	-0.3

The theoretical capacity is calculated based on a two-electron transfer redox process for each formula unit. The detailed electrochemical redox mechanism is shown in Section 3.3.

3.2 Equipment

The name, type and function of some of the equipment used in experiments are listed in the Table 3.2 below.

Table 3.2 Some equipment used during experiments

Name	Type	Function
Analytical Balance	CPA225D	Weighting
Precision Disc Cutter	T-06	Current collector disc cutting
Hot Plate with Magnetic Stirrer	C-Mag HS 7	Heating and stirring
Rotary Evaporator	RV-10	Solvent evaporation
Vacuum Oven	DZF-6050	Drying

Table 3.2 (continued)

Split Tube Furnace	OTF-1200X	Heating
Handheld UV Lamps	UVGL-58	TLC analysis
Nuclear Magnetic Resonance	N/A	Structure analysis
Fourier Transform Infrared Spectrometer	iD5/iS5	Functional groups analysis
Scanning Electron Microscope	N/A	Morphology analysis
Desk-Top Powder Presser	YLJ-24T	Electrode Pressing
Compact Hydraulic Crimping Machine	MKS-110	Coin cell sealing
M. Braun Glove Box Systems	MB10	Coin cell assembly and Dry storage
Landhe Battery Testing System	CT2001	Coin cell testing
Electric Crimper Machine	MSK-160D	Coin cell disassembly

During all synthesis procedures, a hot plate (Figure 3.1a) was always used in the first step for heating and stirring the mixing materials, which include a precursor and a linker. During the second step, the polymers need a tube furnace (Figure 3.1b) to get final product. A rotary evaporator (Figure 3.1c) was used in the synthesis experiment of monomers to remove solvents from samples efficiently and to get intermediates.

**Figure 3.1 (a) Hot Plate (b) Tube Furnace (c) Rotary Evaporator (d) Vacuum Oven**

Generally, in the process of exploring how to synthesize materials, a UV lamp (Figure 3.2e) was used to do thin layer chromatography (TLC) analysis. TLC analysis is a technique used to separate the components of a mixture and therefore monitor the process of a reaction. When I got the final product, SEM technique was used to analyse the morphology of the material, FT-IR method (Figure 3.2d) was used to analyse functional groups of the material, and NMR was used to analyse the structure of the material. These technologies were used to help me find out if the product was the material I want and how pure it was when compared with the target materials.



Figure 3.2 (a) Precision Disc Cutter (b) Desk-Top Powder Presser (c) Analytical Balance (d) Fourier Transform Infrared Spectrometer (e) Handheld UV Lamps

Figure 3.2a shows a precision disc cutter, which was used to cut the stainless steel mesh into a round disc and Figure 3.2b is a press used to press the electrode material into stainless steel mesh when I need a thick electrode. However, most of the time I used a thin electrode and pinched the electrode material with a current collector by using a stainless steel roller.



Figure 3.3 (a) Compact Hydraulic Crimping Machine (b) Electric Crimper Machine (c) Glove Box Systems (d) Landhe Battery Testing System

After the electrodes (mixed slurry and current collector) had dried in the vacuum oven (Figure 3.1d), the coin cell was assembled and sealed by using a compact hydraulic crimping machine (Figure 3.3a). Sometimes, the electrode was tested in organic electrolyte because it can help me find out whether the problem is about the electrode material or electrolyte. In this case, the coin cell was assembled in a glove box system (Figure 3.3c) since both lithium and organic electrolyte hate oxygen. At last, the coin cell

was tested by using a Landhe battery testing system (Figure 3.3d) to get all the performance data of the cell. When a cell shows a bad or unexpected result, it may be disassembled by a de-crimper machine (Figure 3.3b) to see what is going on inside the cell during the charging and discharging process.

3.3 Synthesis

The basic mechanism of these four reactions is based on the imidization reaction. The mechanism of the thermal imidization of solid-state polyamic acid was studied by Y. Xu and Q.H. Zhang [66]. It is assumed that two isomers exist in a polyamic acid segment: one is called the para-segment, which favors imidization reaction; the other is the meta-segment, which is not in favor for imidization unless the temperature is high enough. The results show that the imidization process differs for the two states of polyamic acid segments. The para-segment is more sensitive to the heat environment for the formation of an imide ring, and it will take several intermediate steps to complete the ring closure with the aid of the solvent. As for the meta-segment, the ring will be closed before the imide formation due to the powerful energy provided in the high-temperature environment, and the ever-increasing chain rigidity and the loss of solvent during the heating process make this path the only option to continue the imidization process.

Typically there are two steps to synthesize polyimide, i.e., solution polymerization and heat treatment. The product of the first solution polymerization step usually contains some units not completely cyclized, called polyamic acid. So the second heating step is necessary to achieve a complete imidization. Moreover, the heat treatment can also remove the residual solvent in the polymer. And a similar reaction procedure occurs to monomers. However, monomers need more purification methods than polymers. As

shown in Figure 3.4, take PNDIE as an example of the synthesis procedure.

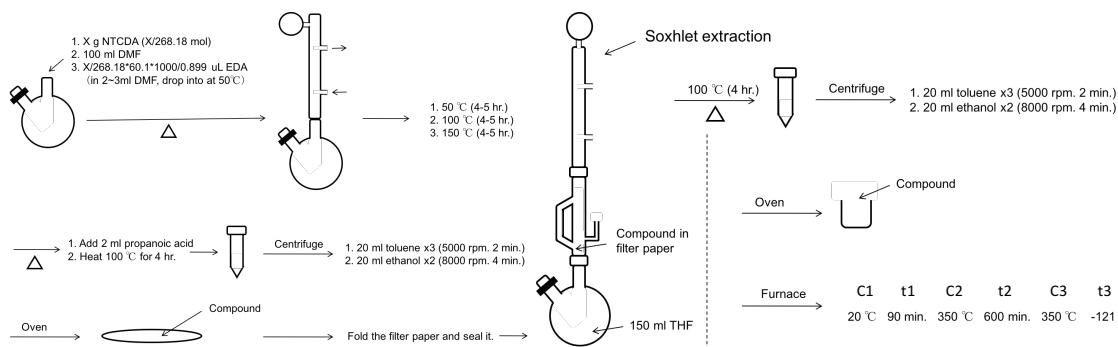


Figure 3.4 PNDIE synthesis procedure

Regarding the mechanism of these four materials, PDIE is an example that shows the mechanism during the reaction in Figure 3.5. From Figure 3.5 we can see after the first step there exists intermediate and after heating in high temperature we can get rid of most of the intermediate and water for the final product. The electrochemical redox mechanism is shown in Figure 3.6.

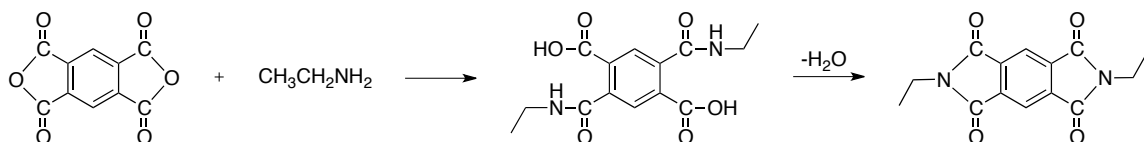


Figure 3.5 Imidization reaction mechanism

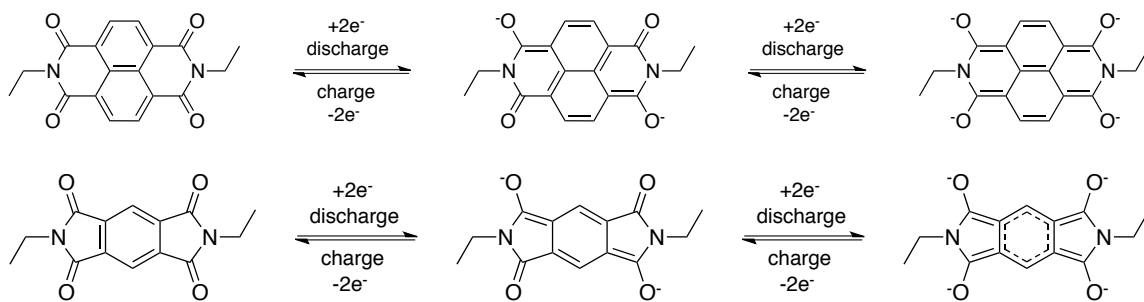


Figure 3.6 Electrochemical redox mechanisms

3.3.1 Monomer

PDIE: Pyromellitic dianhydride (2.18 g, 10 mmol) and n-ethylamine (30 mL, 70%

v/v) was mixed together and stirred in a sealed vessel at 80°C for 7 hours. The resulting solids were filtered off and dried in the oven at 100°C for 3 hours (white solid, 1.91 g). Then sublimation further heated the intermediate and re-crystallization improved the purity of the product (white crystalline substance, 545 mg).

NDIE: A brown suspension of naphthalene-1,4,5,8-tetracarboxylic dianhydride (2.68 g, 10 mmol) in aqueous n-ethylamine (30 mL, 70% v/v) was stirred in a sealed vessel at 90°C overnight and then the solvent (water) was removed by evaporation, leaving behind the undissolved substance. Then, the salt bath heating method (350°C) was used to get the final product (2.54 g).

The synthesis method provided above is still under study and needs to improve through further experiments. The yield of NDIE has already been increased from 11% to 78.8% and the yield of PDIE from 2% to 20%. Since I varied the synthesis methods, the color of the final product varied from pink to orange to black. Figure 3.7 shows NDIE in an orange color and PDIE in a white color. The synthesis equations for monomers are given below in Figure 3.8.

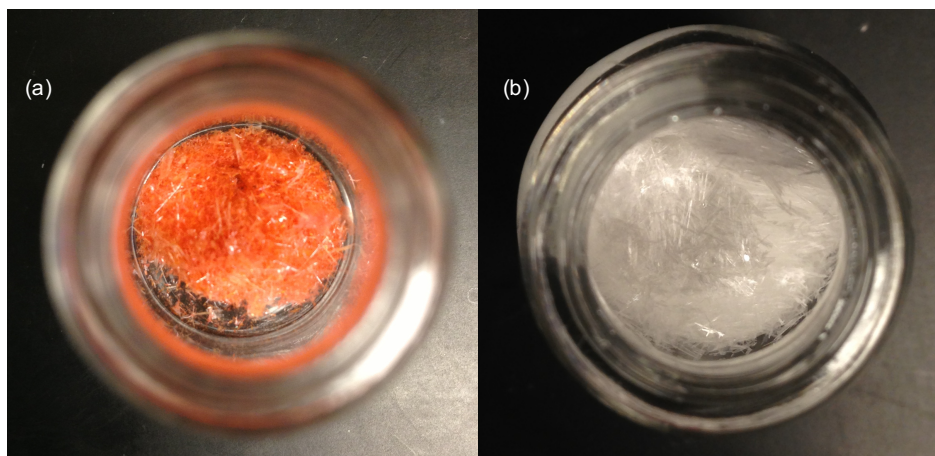


Figure 3.7 (a) NDIE (yield: 78.8%) (b) PDIE (yield: 20%)

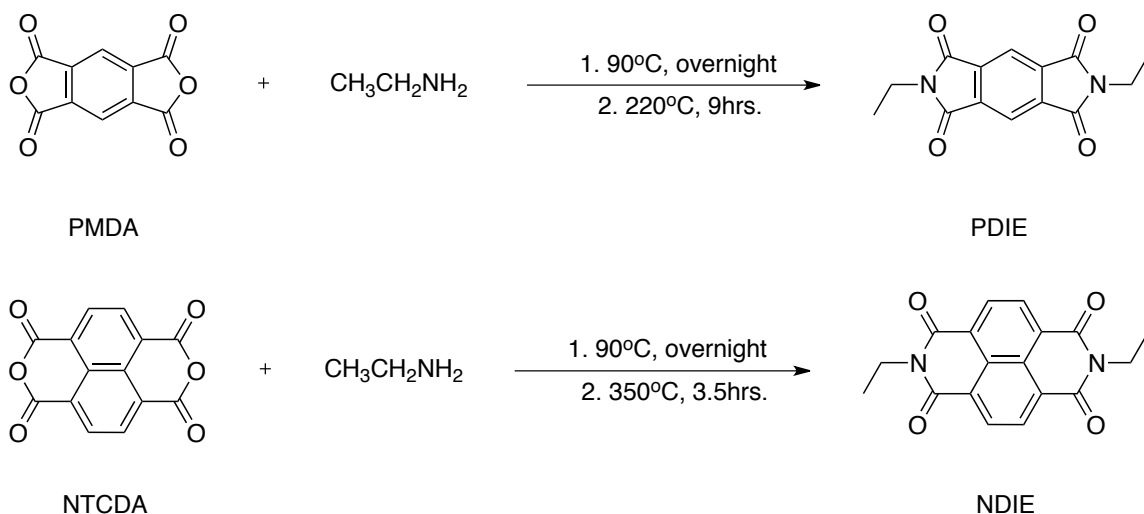


Figure 3.8 Reaction equations for monomers

3.3.2 Polymer

PPDIE: PMDA (96.6 mg) and EDA (ethylene diamine, 0.03 ml) reacted under reflux in DMF (13 ml) for 6 hours; the product was filtrated, washed with ethanol several times, dried at 120°C in air for 9 hours, then heated in Nitrogen for 11.5 hours at 350°C.

PNDIE: NTCDA (2.15 g), EDA (0.53 ml) and 150ml DMF was mixed together and stirred under reflux overnight. The temperature was increased from 50°C to 150°C gradually. Then the intermediate was washed with toluene and ethanol (three times each) by using a centrifuge. After drying at 120°C in an oven for four hours, the product was then heated in argon for 11.5 hours at 350°C.

The synthesis method for PNDIE is relatively more mature than for PPDIE; therefore we achieved an 85.9% yield of PNDIE, which has a rather good performance in battery, and for PPDIE the yield is 73.8%. Both PNDIE and PPDIE have a brown color (Figure 3.9). The reaction equations for both polymers are given in Figure 3.10.

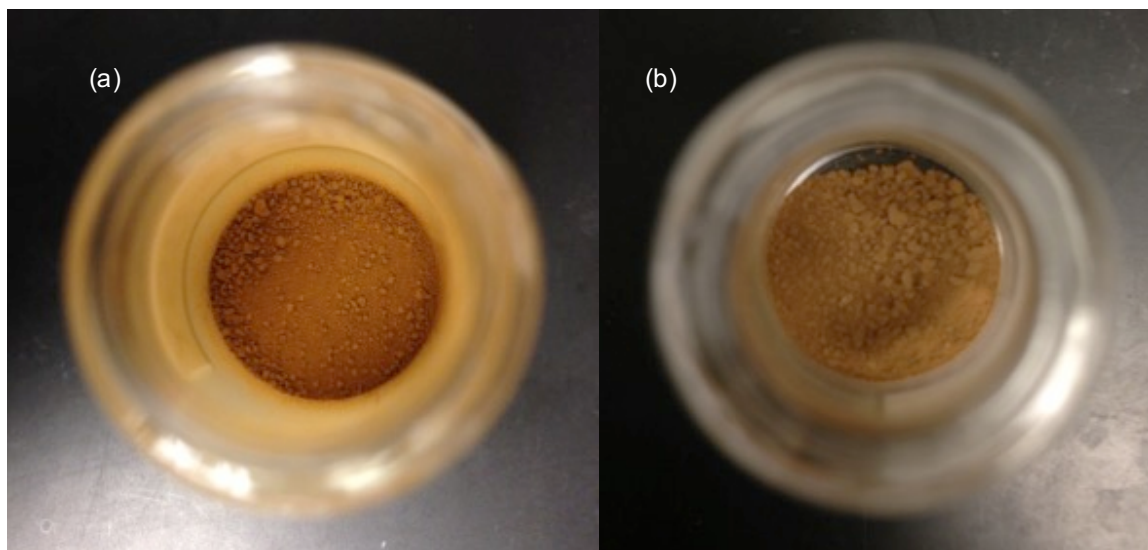


Figure 3.9 (a) PNDIE (yield: 85.9%) (b) PPDIE (yield: 73.8%)

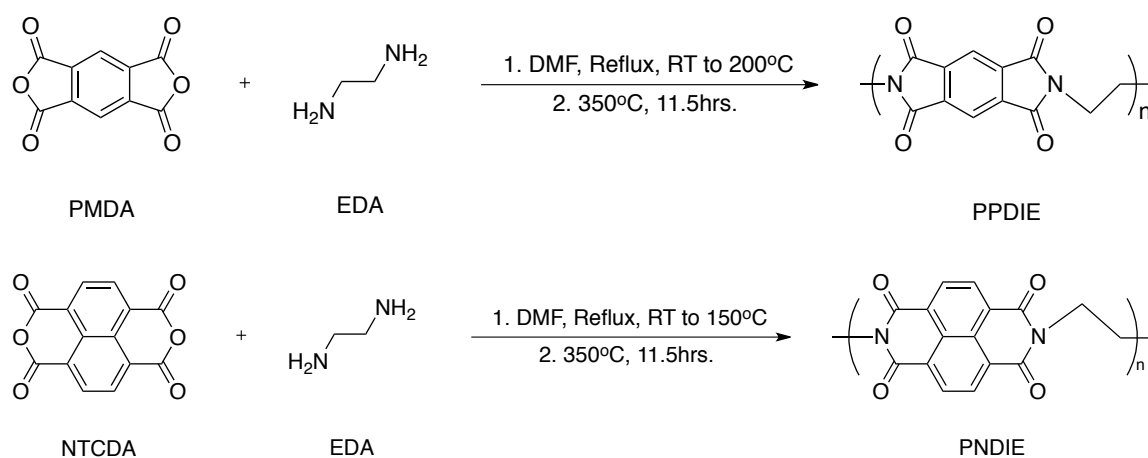


Figure 3.10 Reaction equations for PPDIE and PNDIE

3.3.3 Challenges for Monomer Synthesis

The actual work towards synthesis is not that simple as we just described in the previous two sections. During the synthesis procedure, a lot of difficulty occurs, especially for two monomers. After the basic synthesis method, other additional procedures, like recrystallization and sublimation, were used to improve the purity or yield of materials. In my work, the problem with NDIE, i.e., low yield, has been

improved a lot. The same problem also happened to PDIE; however, only a little improvement has been made.

3.3.3.1 NDIE

I got very low yield from the first three batches. I kept changing the reaction vessel from the first batch, which is Batch 1-75 (meaning the first experiment note book, page 75), to the second batch (1-86), and to the third batch (1-88) because I thought the problem was mainly due to the leaking problem and the reaction temperature was not high enough to complete the reaction. The results showed not much difference. That means I have to try another heating method after the first step, not just change a vessel. So I tried a series method to deal with 1-88 NDIE and finally I found out the salt bath was a good way. At last, the 4th batch was synthesized and finally got an obviously better result. The detailed experimental procedure used to get the third batch of NDIE, Batch 1-88, was shown in Figure 3.11 below.

Among all the attempts I have tried for getting more pure NDIE, salt bath sublimation is the best method. The reasons are: (1) compared with oil bath sublimation, it can reach higher temperature; (2) compared with hot ethanol extraction, it has higher yield and an easier process (22.5% vs. 54.5%); (3) compared with sand bath sublimation, it has a safer and easier process because sand has a higher melting point (1713°C vs. 250°C) and cannot get evenly heated during the process (finally need 350°C in my case). The salt I used in the experiment was a mixture of half sodium nitrate and half potassium nitrate in weight. The operation temperature for this salt mixture is 260°C-550°C. It is perfect for my experiment, which requires 350°C in the end.

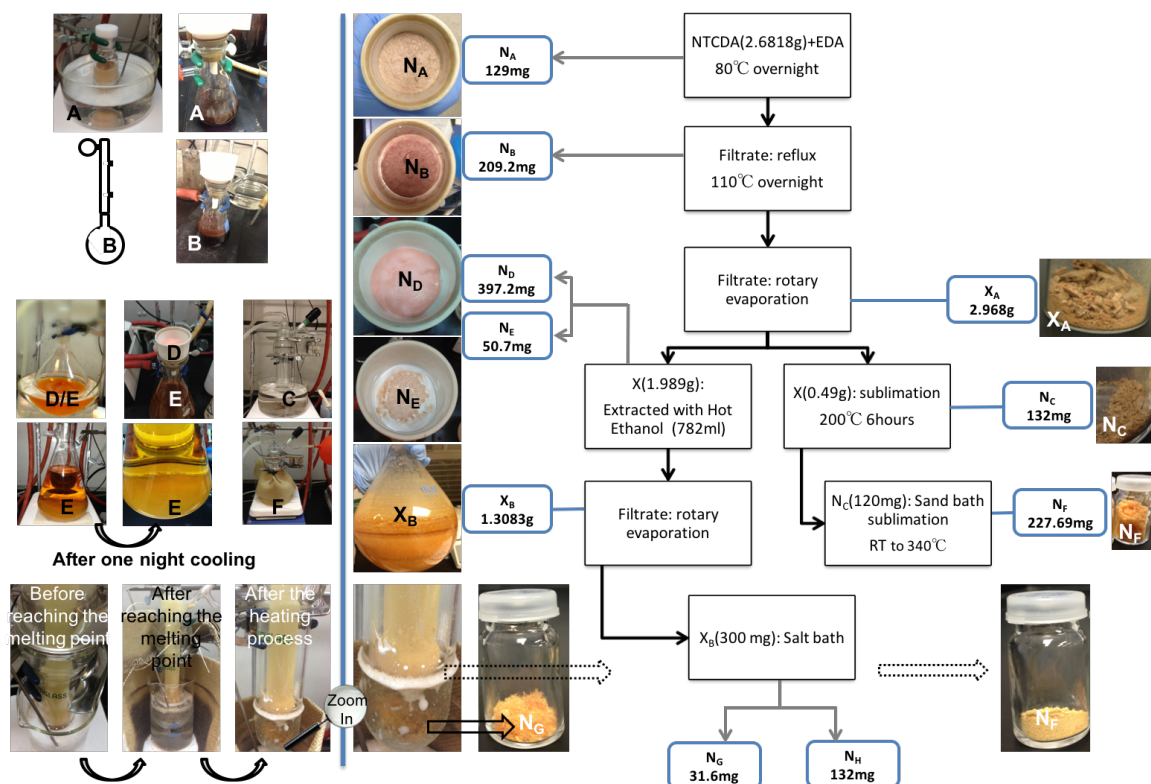


Figure 3.11 Different attempts on 1-88 NDIE for improving the yield

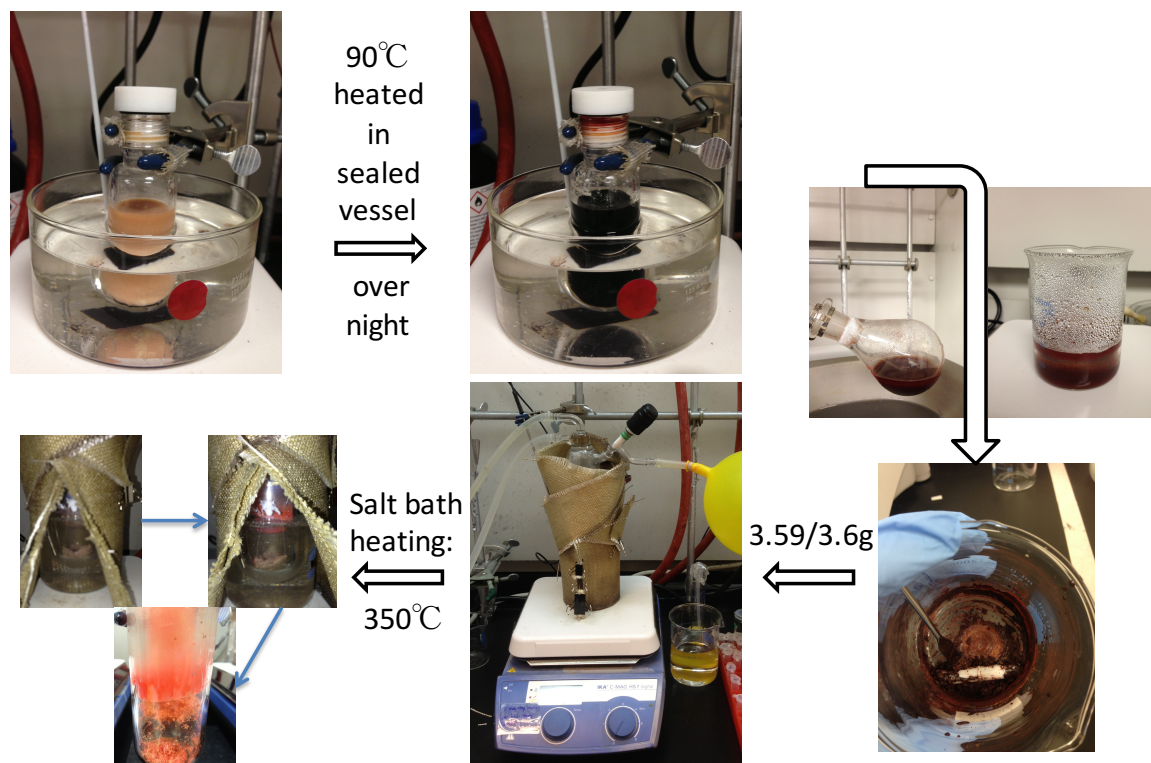


Figure 3.12 Synthesis procedure for 1-99 NDIE

After determining the synthesis plan, the last batch of NDIE (1-99) was synthesized. The Figure 3.12 shows the synthesis procedure of 1-99 NDIE. According to the position of products inside the sublimation chamber, they were divided into three parts, N_A , N_B and X_A . After testing them in TLC, NMR and IR, all of them can be defined as NDIE. Detailed information can be found in the figure below.

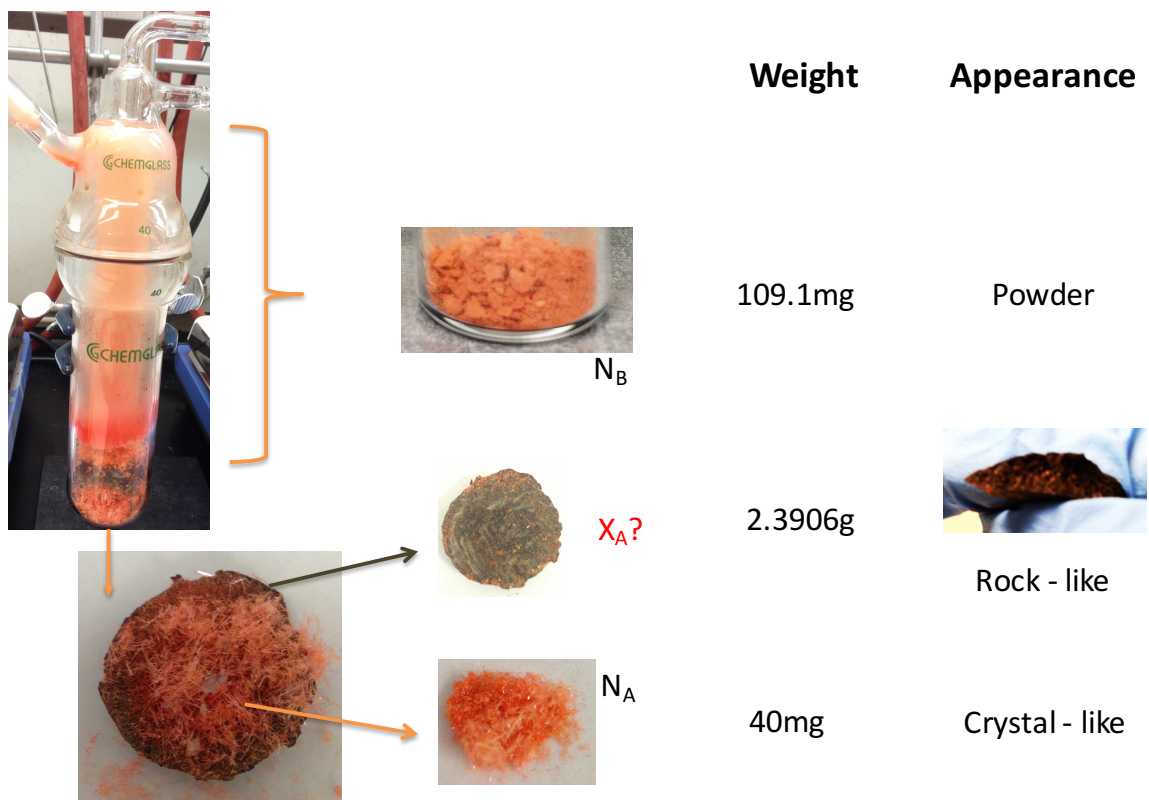


Figure 3.13 Information about the products from different position of sublimation chamber

3.3.3.2 PDIE

Similar with NDIE, PDIE also has the yield (about 20%) problem and purity problem. However, I only improved the purity of PDIE but did not solve the yield problem. After the first batch of PDIE (1-78), I tried sublimation and recrystallization to get rid of the impurity. Recrystallization seemed to work very well. The Figure 3.14 shows how I did recrystallization and got clean crystal substance, i.e., 1-81 PDIE.

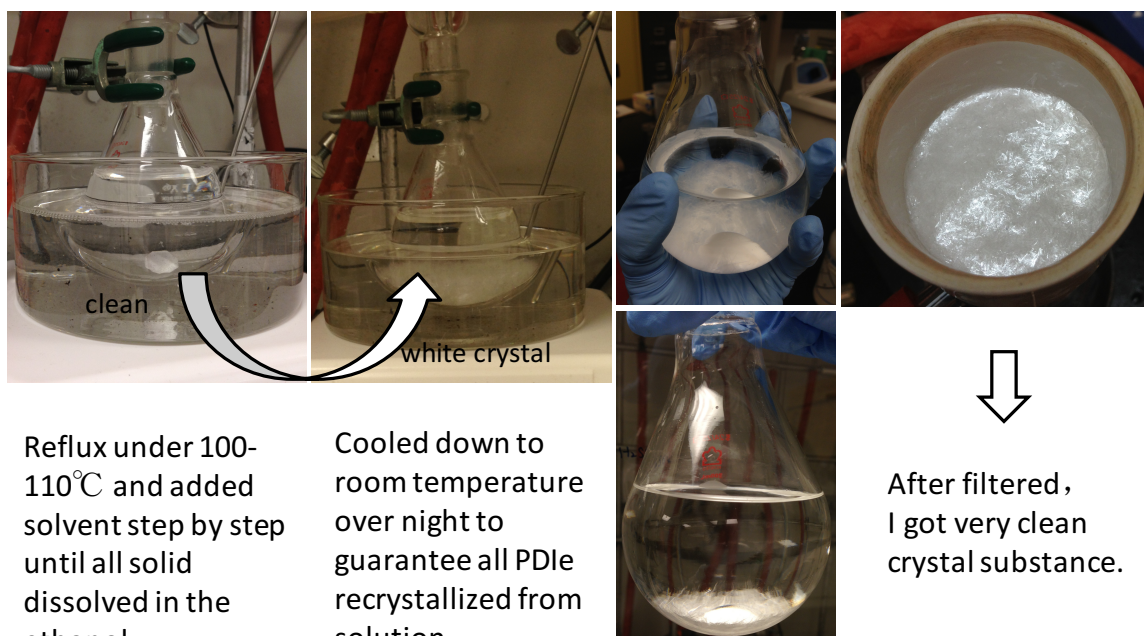


Figure 3.14 Recrystallization procedure of 1-81 PDIE

Chapter 4 Cell Fabrication and Characterization

4.1 Cell Fabrication and Electrode Preparation

4.1.1 Cell Fabrication

The coin cell was fabricated to investigate the electrochemical performance of the electrode material. Figure 4.1 shows a basic procedure of coin cell fabrication (using LMO as cathode material for example). When testing materials in an aqueous system, I usually use active carbon as the counter electrode, 2.5 M Li_2SO_4 (pH=7) as the electrolyte, glass fiber as the separator, and 1 C as the c-rate. Mass loading is about 0.5-1.5 mg.

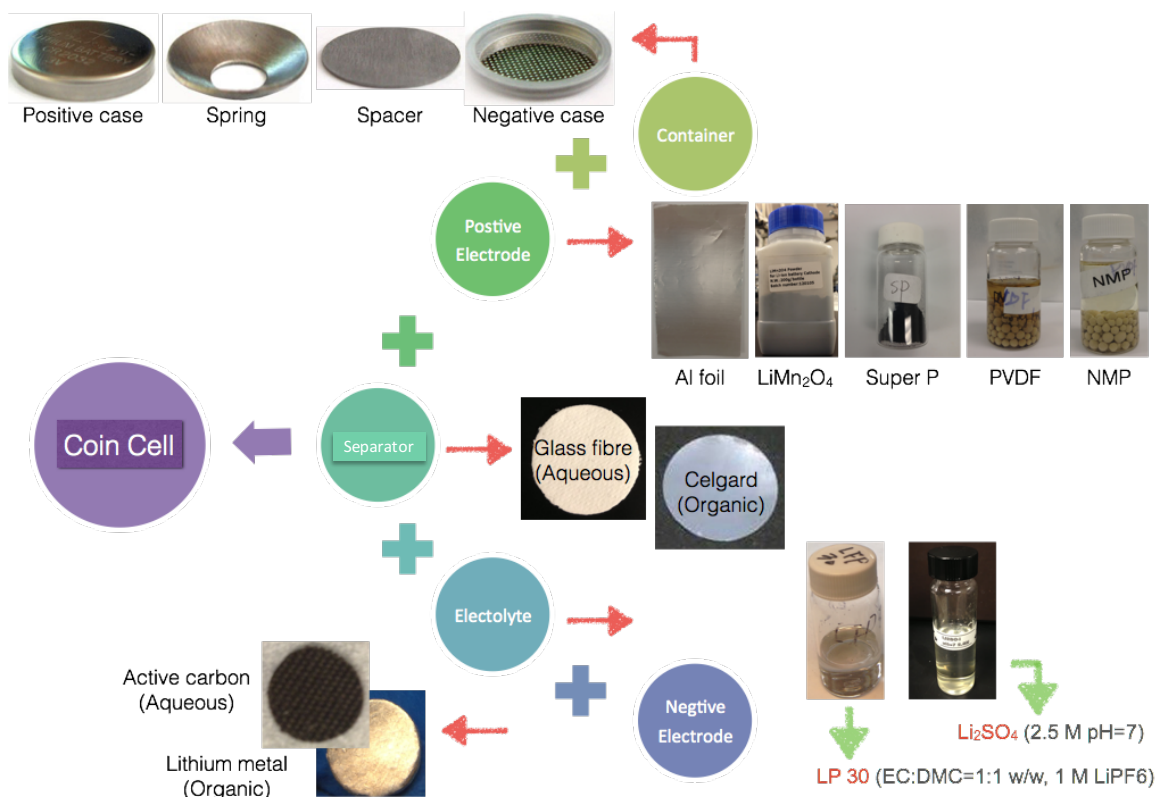


Figure 4.1 Coin cell fabrication

4.1.2 Electrode Preparation

The electrode preparation using four different active materials was conducted in a similar way. The electrode was prepared by pressing a powdered mixture of the sample, super P, and poly(tetrafluoroethylene), in a weight ratio of 60:30:10. After they evenly mixed by using an agate mortar and pestle, the electrode disks were pinched into stainless steel meshes.

4.2 Physical and Structure Characterizations

We have used several characterization techniques to study the materials, such as TLC to monitor the progress of a reaction, NMR to identify the structure and purity, IR to identify functional groups, SEM to study the morphology and particle size, and XRD to study crystallinity. Some testing results are presented in the following figures.

4.2.1 Nuclear Magnetic Resonance

Nuclear Magnetic Resonance (NMR) Spectroscopy can be used to analyse the local electronic interactions of a nucleus by using the electromagnetic radiation of radio waves. Therefore, it was used in my study to confirm the identity of a substance by comparing the positions, intensities (area ratio), and fine structure (splitting) of resonance peaks between the target materials and my materials. Also, from the comparison, we can determine how pure my materials are. Since two polymers I synthesized are insoluble and it is very difficult to get solid-state NMR testing (no solid-state NMR machine in UH), I only have NMR results for two monomers here.

In Figure 4.2, the top one shows the NMR for NDIE and the bottom one shows the NMR result for PDIE. Result details: ^1H NMR (400 MHz, CDCl_3 , NDIE): 1.34 (6.14H), 4.26 (4.21H), 8.74 (4H); ^1H NMR (400 MHz, CDCl_3 , PDIE): 1.31 (6.02H), 3.8 (4.18H),

8.26 (2H). Comparing the NMR result of NDIE with the reference [56], the position of all three peaks are exactly the same. Also, there is a tiny peak next to position 1.31 that has an integral of 0.92 (not ignorable), which leads to an unknown impurity. Regarding PDIE, there is no reference data to compare. From the data I collected, it can be concluded that the singlet peak at 8.26 ppm corresponds to the two hydrogen attach to the benzene ring, the quadruplet peaks at 3.8 ppm corresponds to the 4 hydrogen in methylene group, and the triplet peaks at 1.31 ppm corresponds to the 6 hydrogen in methyl group.

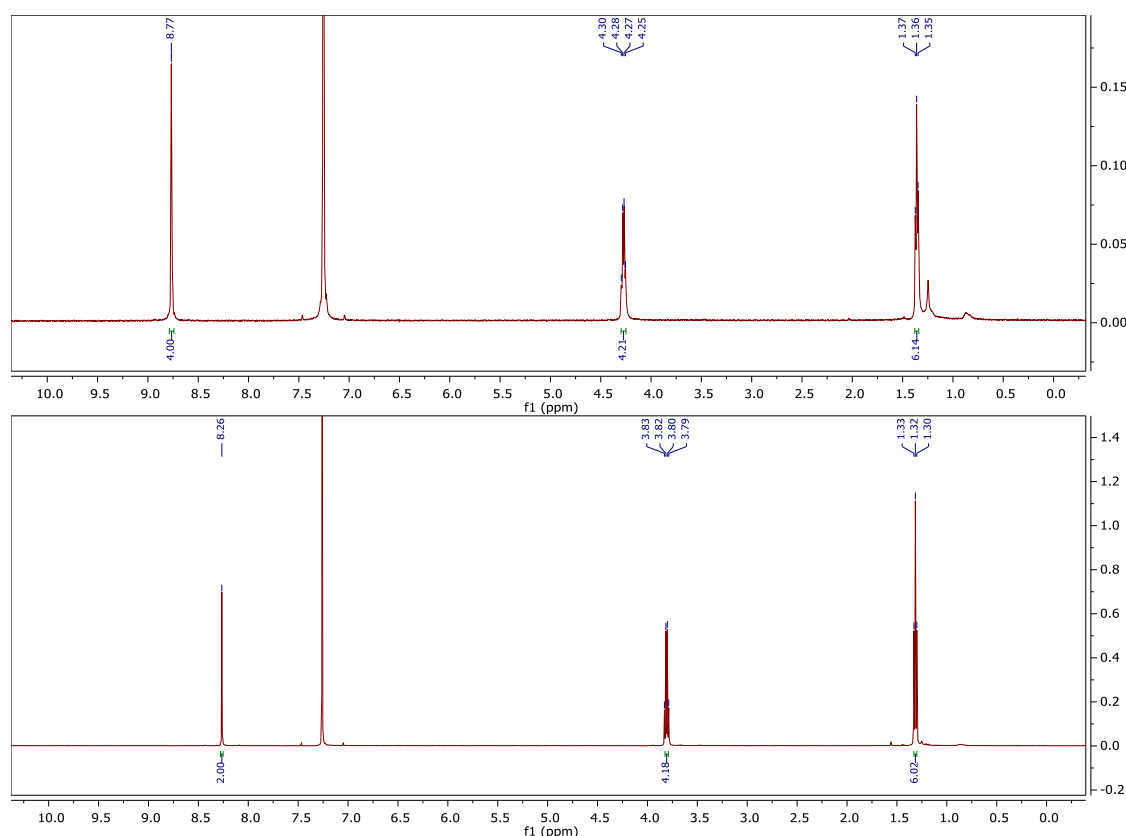


Figure 4.2 NMR spectrum of NDIE and PDIE

4.2.2 Fourier Transform Infrared spectroscopy

Infrared Spectroscopy can be used to analyze a molecule by using infrared light interacting with the molecule. In my work, the products were structurally characterized

by ATR-FTIR spectroscopy. It was used to determine functional groups in molecules. IR Spectroscopy measures the vibrations of atoms, and based on this it is possible to determine the functional groups. Generally, stronger bonds and light atoms will vibrate at a high stretching frequency (wavenumber).

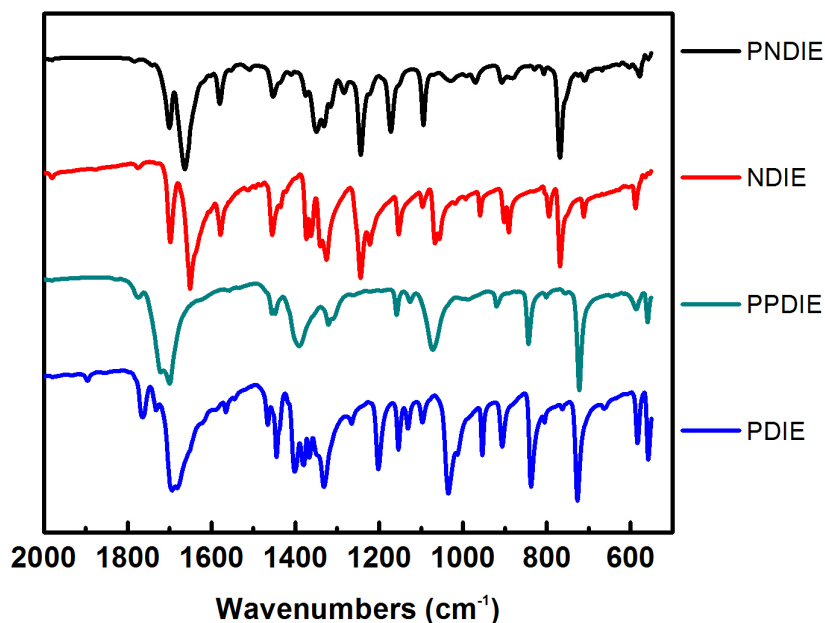


Figure 4.3 IR spectroscopy of PNDIE, NDIE, PPDIE and PDIE

In general, IR spectra (Figure 4.3) for PNDIE and NDIE resemble each other when wavenumbers are higher than 1400. IR bands are assigned in Table 4.1 below. The literature values of PI-4 and PI-2 [61] (shown as PNDIE^[61] and PPDIE^[61] in the table) were used as a reference for PNDIE and PPDIE in my work.

Table 4.1 Characteristic IR band assignments of the four samples

Group	PDIE	NDIE	PNDIE	PPDIE	PNDIE ^[61]	PPDIE ^[61]
imide C=O, ν_{as}	1764	1698	1700	1774	1703	1774
imide C=O, ν_s	1694	1651	1663	1699	1670	1722
imide C-N, ν	1332	1326	1350	1390	1350	1388
imide C=O, δ	727	769	769	722	7711	726

4.2.3 Scanning Electron Microscope

Scanning electron microscopy (SEM) is a type of electron microscope. It is more like a mapping device, using a beam of electrons scanning across the surface of the sample creating the overall image. In my work, it was used to characterize the morphology and detailed structure of samples.

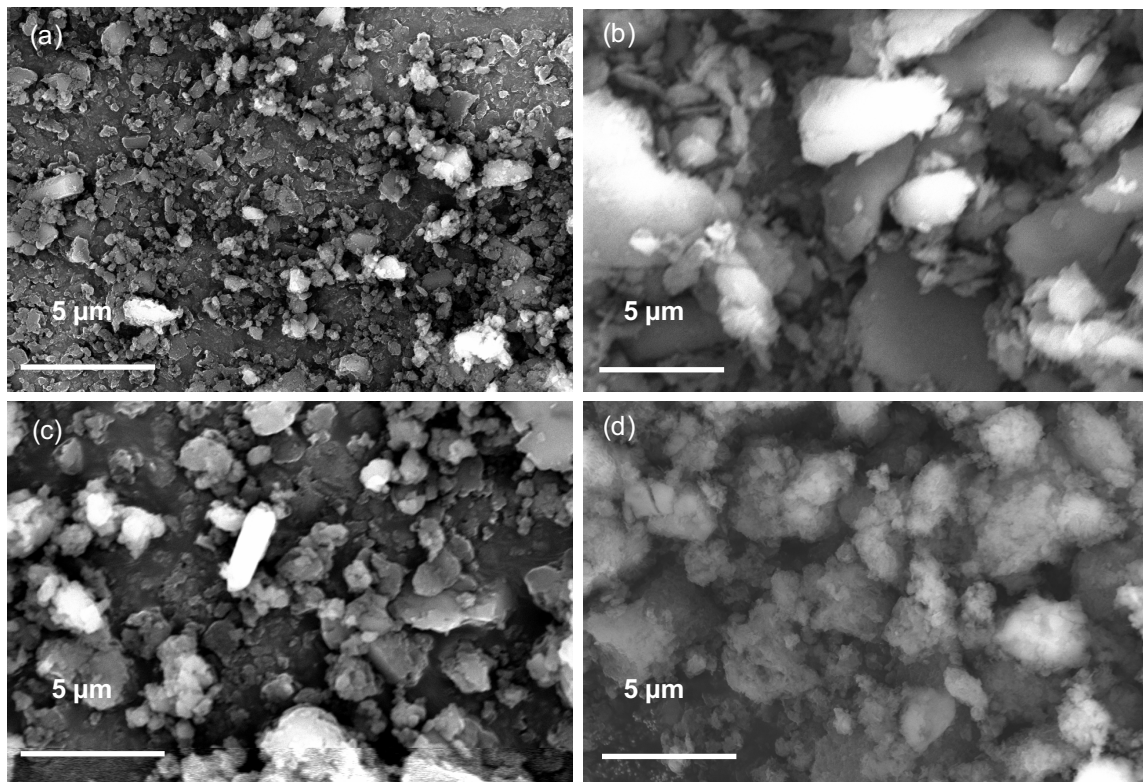


Figure 4.4 SEM Image of (a) NDIE (b) PDIE (c) PNDIE (d) PPDIE

Figure 4.4a displays that NDIE is composed of nanoparticles and micro-particles; the diameter of single particle ranges from 100 nm to 2 μm. Interestingly, a few micro-rods with hexagon profile can be also found in the sample. Figure 4.4b displays that PDIE is also composed of nanoparticles and micro-particles; however, the diameters of many particles are larger than those of NDIE ($>2\text{ }\mu\text{m}$).

Figure 4.4c displays that PNDIE is composed of nanoparticles and micro-particles, but the sizes of the particles become larger than those of NDIE during polymerization. Figure 4.4d clearly shows that PPDIE is composed of aggregated particles. The diameters of the aggregated particles are in the range of 2-5 μm .

4.3 Electrochemical Measurements

4.3.1 Cyclic Voltammetry (CV)

Cyclic voltammetry (CV) is a type of potentiodynamic electrochemical measurement used for studying electrochemical reactions. It has been a popular tool since several decades ago [67]. Organic chemists have applied the technique to the studies of simple redox pathways in both organic and inorganic chemistry and to the characterization of multi-electron-transfer processes in biochemistry and macromolecular chemistry [68]. In a CV test, the cell is cycled in a specified potential window (e.g. E_I - E_S). Starting from an initial potential E_I , a linear potential sweep is applied to this electrode and after reaching a switching potential E_S the sweep is reversed and the potential returns linearly to its initial value. These cycles of ramps in potential may be repeated as many times as wanted. At last, the cyclic voltammetry trace will be plotted containing the current at the working electrode versus the applied voltage.

CV was used in this research work to study the electrochemical properties of electrodes made from different as-prepared materials. CV curves of NDIE and PDIE in 2.5 mol/L Li_2SO_4 aqueous electrolytes are shown in Figure 4.5. At the low scan rate of 1 mV/s, there are two well-defined peaks for PDIE located at -0.423 and -0.62 V vs. SHE, and -0.528 and -0.737 V vs. SHE, respectively, corresponding to the oxidation and reduction reaction. For NDIE, there are three couples of peaks located at -0.08/-0.318, -

0.282/-0.417, and -0.464/-0.6 V vs. SHE. In addition, there is a small peak at -0.357 V and it disappears after the 8th cycle. The reason why this small peak exists needs further study.

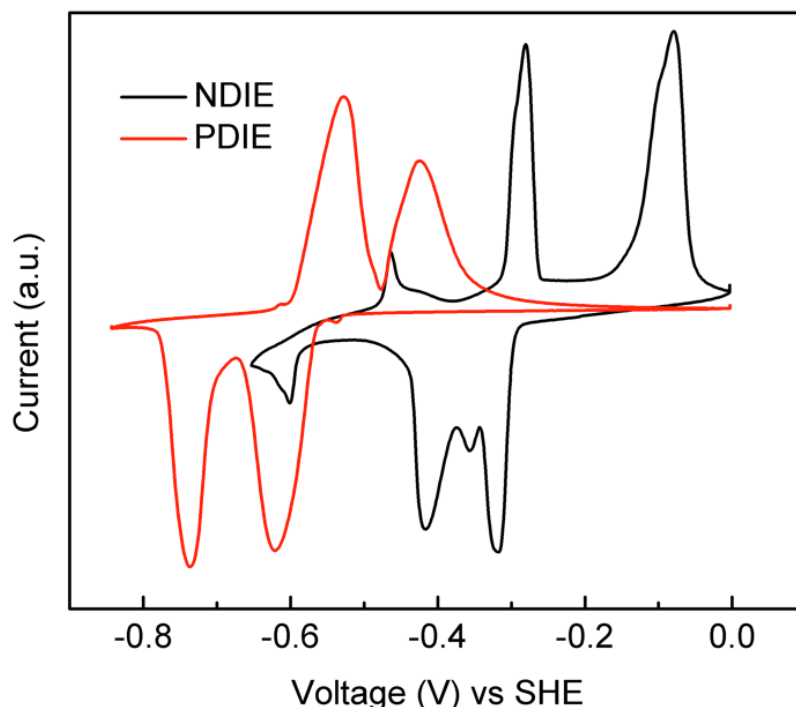


Figure 4.5 Cyclic voltammetry of NDIE and PDIE at the scan rates 1 mV/s

4.3.2 Galvanostatic Charge and Discharge Testing

Charge and discharge cycles of the coin cells were measured using various voltage cut-offs on a Land battery test system at the different constant C-rates. During galvanostatic cycling of batteries, the charge and discharge current are often expressed as a C-rate calculated from the battery capacity.

4.3.2.1 Overall and Comparison Result

Figure 4.6 shows the charge and discharge curves, corresponding efficiencies, and cycling performances. Figure 4.6 a/b shows PDIE, Figure 4.6 c/d shows NDIE, and Figure 4.6 e/f shows PNDIE. From Figure 4.6 we can see that there is only one plateau in

PNDIE and there are 2 and 3 plateaus in PDIE and NDIE, respectively. From the cycling performance we can see PDIE decays very fast, NDIE decays slowly, and PNDIE shows very good stability and very high retention after 100 cycles.

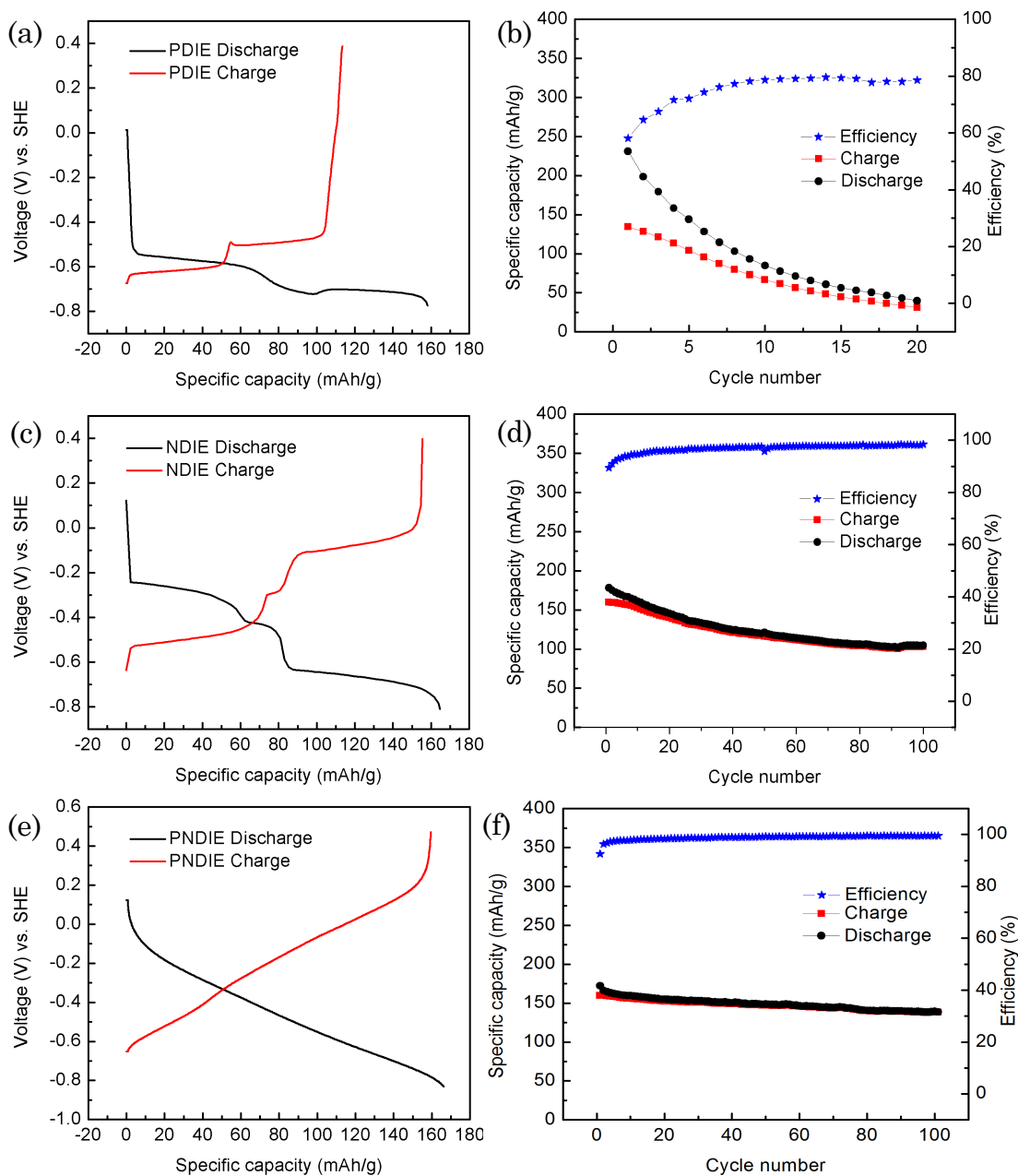


Figure 4.6 Charge/discharge curves of (a) PDIE (c) NDIE (e) PNDIE and cycling performance of (b) PDIE (d) NDIE (f) PNDIE. Cutoff voltages for (a) - 0.8 – 0.4 V; (c) -0.8 – 0.4 V; (e) -0.85 – 0.45 V.

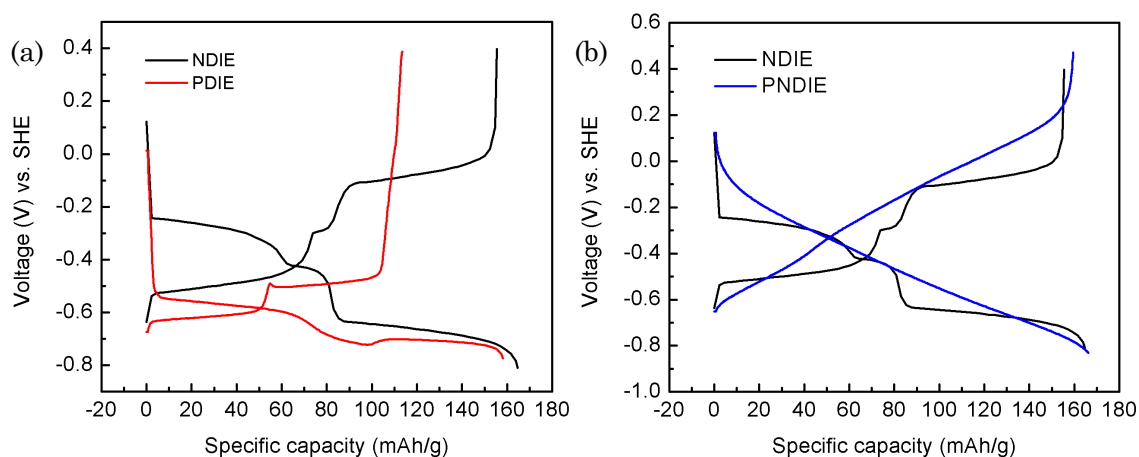


Figure 4.7 Charge/discharge curves of (a) NDIE & PDIE (b) NDIE & PNDIE

The comparison for the monomer (PDIE/NDIE) and the NDI-based compound (PNDIE/NDIE) are shown in Figure 4.7 above. In Figure 4.7, the difference of redox potential for PDIE and NDIE is about 0.2V (-0.577 vs. -0.388), and for NTCDA derived material is 0.065V, which are in accordance with the result from CV testing. In addition, NDIE has a much better coulombic efficiency than PDIE with similar discharge capacity.

4.3.2.2 Progress of NDIE

After having a better yield in synthesis, there was also a need for improving the performance of the cells. The major problem for the NDIE coin cell was the active material dissolved in the electrolyte. For slowing down the decay of specific capacity, I want to trap the dissolved NDIE during cycling. The basic idea is using a normal size carbon paper (CP) as the current collector and using an additional bigger size CP between the electrode and the separator. Because the CP has a more compact structure than the stainless steel mesh, some of dissolved material can be trapped between the current collector and this additional CP, and therefore slow down the capacity loss. The diagram of this new designed coin cell is shown in Figure 4.9 and the improved cycling performance is shown in Figure 4.8.

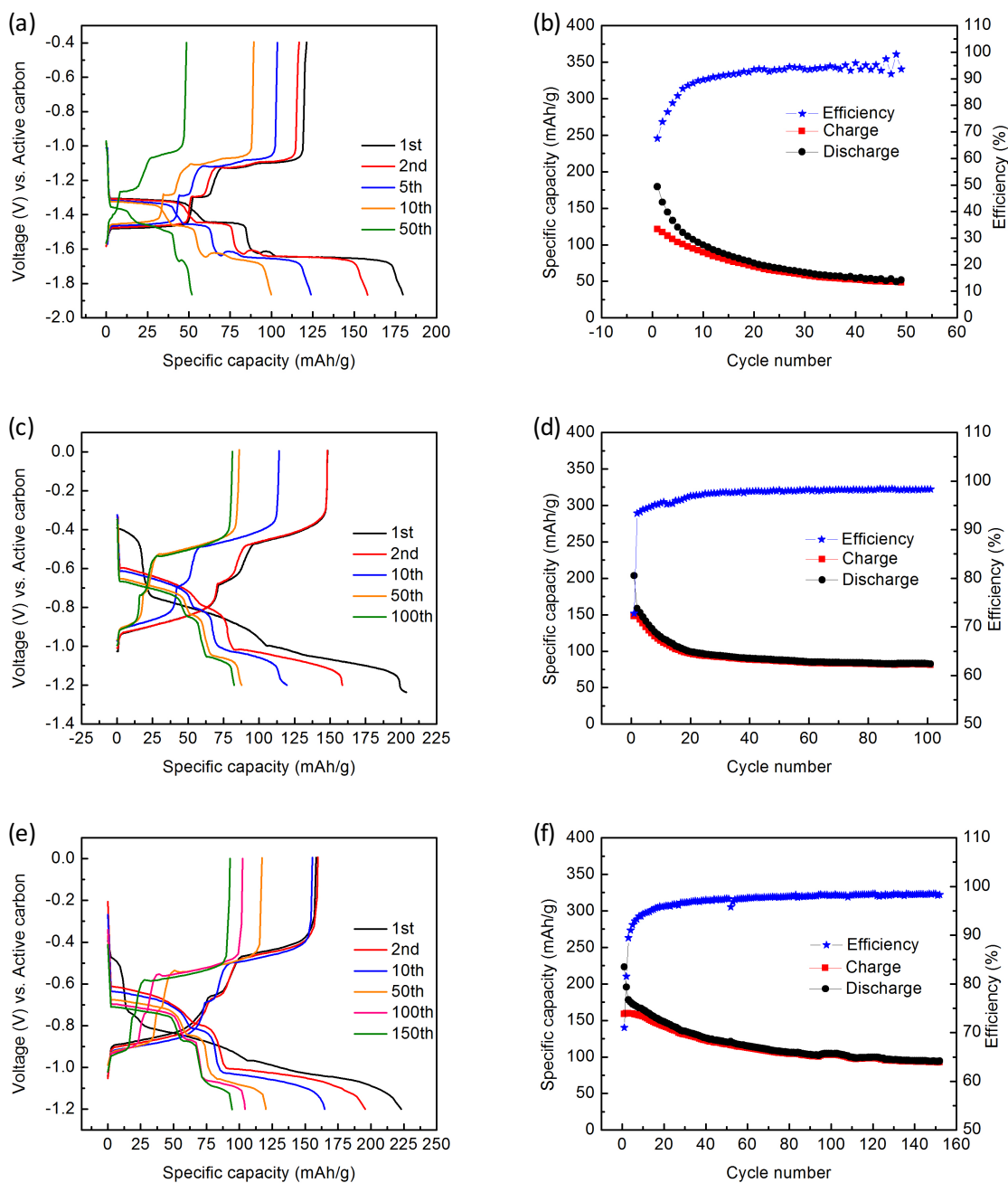


Figure 4.8 (a)/(c) Charge/discharge curves of NDIE coin cell (b)/(d) Corresponding cycling performance and coulombic efficiency curves ((a)/(b) without CP (c)/(d) with regular CP (e)/(f) with large CP)

Figure 4.8 shows the electrochemical performance of the NDIE cell under the different conditions. When no additional carbon paper was used in coin cell fabrication, the cell got 85.4%/73.7%/57.7%/39.9% retention after 5/10/20/50 cycles, respectively.

When an additional regular size CP was used in coin cell fabrication, the cell got 89.8%/77%/65%/58%/54.9 retention after 5/10/20/50/100 cycles, respectively. When an additional large size CP was used in coin cell fabrication, the cell got 100%/97.7%/89.4%/73.7%/64.6%/58.3% retention after 5/10/20/50/100/150 cycles, respectively. From the data we can see that after a regular size CP was used, very little improvement has been made, while after a large CP was used, great improvement has been made. So it is more successful to trap the dissolved materials by using the large CP. An obvious improvement is shown in Figure 4.10.

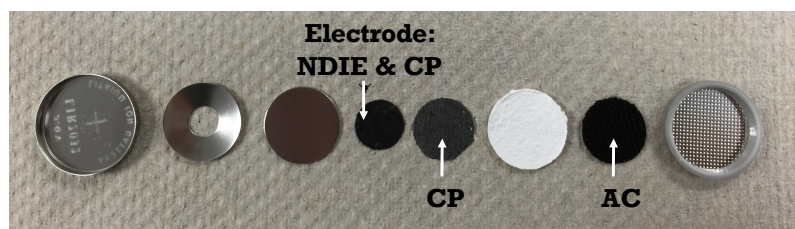


Figure 4.9 Schematic diagram of new designed coin cell for NDIE

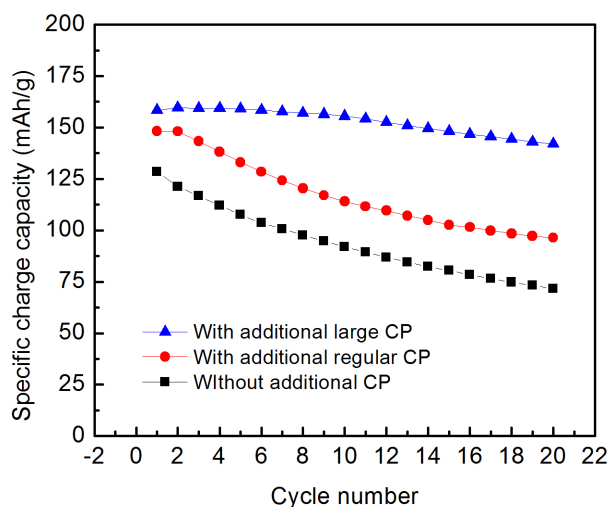


Figure 4.10 A comparison of cycling performance of NDIE coin cells

4.3.2.3 Long Cycle Stability of PNDIE

In my work, PNDIE has the best performance all the time. Figure 4.11 shows PNDIE^{1st}, namely the first batch PNDIE, can reach 159.5 mAh/g when charging in its first cycle and 91.8%/86.5% retention after 50/100 cycles. Figure 4.12 shows PNDIE^{2nd},

namely the second batch PNDIE, can reach 117.8 mAh/g and 95.2%/82.9% retention after 50/500 cycles. The good stability and high coulombic efficiency of PNDIE shows good reaction reversibility of the imide group and stable polymer framework, which make it a promising anode electrode material candidate for ALIBs.

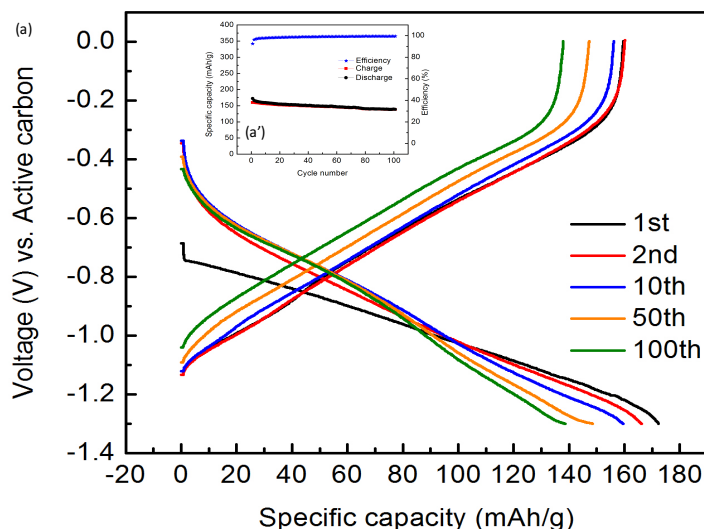


Figure 4.11 (a) Charge/discharge curves of PNDIE^{1st(1-8)} coin cell (a') Corresponding cycling performance and coulombic efficiency curves

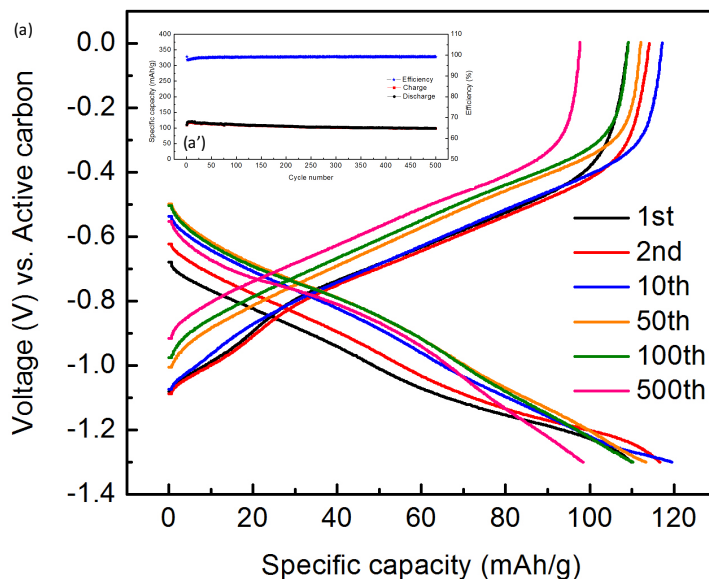


Figure 4.12 (a) Charge/discharge curves of PNDIE^{2nd} coin cell (a') Corresponding cycling performance and coulombic efficiency curves

4.3.2.4 Fast fading in PDIE's cycling life

Although after adding one carbon paper in the PDIE cell also improved the performance a little bit, the capacity-fading phenomenon still exists. From Figure 4.13a/b we can see, before using the carbon paper, obvious capacity fading starts from the second cycle, only 79.3% retention compared with the first cycle. Also, only 40.4% specific capacity remains after the 5th cycle and 3% after the 50th cycle. However, after using the carbon paper, we can get 99.5% retention after the 2nd cycle and 83.9% after the 5th cycle. Nevertheless, only 7.6% remains after the 50th cycle, which is not much different when compared to the non-CP PDIE coin cell.

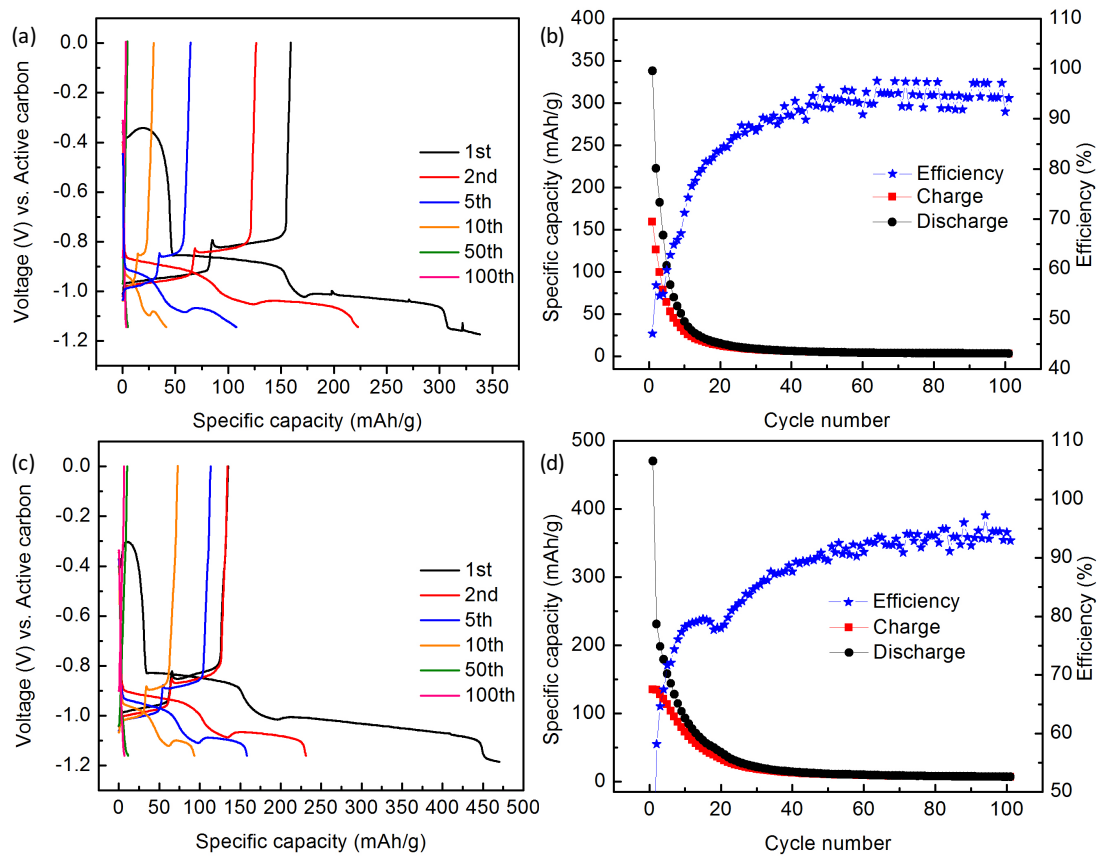


Figure 4.13 (a)/(c) Charge/discharge curves of PDIE coin cell (b)/(d) Corresponding cycling performance and coulombic efficiency curves ((a)/(b) without CP (c)/(d) with CP)

Chapter 5 Conclusion and Summary

5.1 Conclusion

The following conclusions can be made in this study:

(1) The super-low yield of the first attempt at monomers synthesis may be due to the high solubility of the intermediate. During the washing process, most of the intermediates were washed away. So after I used evaporating to remove the solvent of the first step instead of washing, the yield increased noticeably, from 2% to 20% for PDIE and from 11% to 78.8% for NDIE.

(2) The fast decay of electrochemical performance for the NDIE coin cell may be due to the active material dissolution in electrolyte. After I changed the current collector from stainless steel mesh to carbon paper and used an additional bigger carbon paper in the middle of the electrode and separator, the cell's performance improved. The specific capacity of NDIE can reach 166.3 mAh/g and 79.8% retention after 50 cycles.

(3) After polymerization of NDIE, PNDIE shows very good electrochemical performance. The specific capacity of PNDIE can reach 159.5 mAh/g at the first cycle, has 91.8% retention after 50 cycles, and has 86.4% retention after 100 cycles. Another cell of PNDIE can reach 117.8 mAh/g and get 95.2% and 82.9% after 100 and 500 cycles, respectively. That is two examples that prove PNDIE can reach high capacity and good cycling performance at the same time. The main reason why PNDIE has better performance than NDIE is because it is insolvable in electrolyte, which effectively avoids the capacity fading caused by active material decreasing.

(4) After using an additional carbon paper in PDIE coin cells, which also have the dissolution problem, the electrochemical performance can only be improved within the

first several cycles. It means either this method is not good enough, the main reason for capacity decay is something else, or both.

(5) Although I slightly improved the yield of PDIE and synthesized PPDIE successfully, I still cannot get very good performance for PDIE and almost no performance for PPDIE. The reason might relate to the different structure of PDI-based materials. Since I didn't really find out what the key reason is and so far no related article has information about PDI-based materials in aqueous electrolyte, future work needs to continue on PDI-based materials.

5.2 Summary

In summary, PDIE/NDIE/PNDIE/PPDIE based coin cells were fabricated in aqueous electrolytes and investigated as anode materials for the lithium ion battery. Imide-based ARLB is cheap in cost, harmless to the environment, easy in assembly and safe in use. Also, it avoids the use of poisonous metals and flammable and harmful acidic or alkaline electrolytes. Last but not the least, each formula unit of the electrode materials is able to transfer at least two electrons through two synthesis steps which may allow a theoretical specific capacity of about 150 mAh/g.

Although the synthetic procedure is quite simple compared to other organic materials, researchers still need lots of efforts to try the different conditions, including solvent, temperature, time, etc. Also, cell fabrication and testing needs lots of attempts, including cell selection (coin cell, three electrode cell, flood cell, pouch cell, etc.); electrolyte selection (salt, concentration, pH, etc.); separator selection (glass fiber, celgard, etc.); current collector selection (stainless steel/Cu/Al/ foil/mesh, etc.); binder selection (PVDF, PTFE, etc.); ratio selection (6:3:1, 3:6:1, 8:1:1, etc.); c rate selection

(0.5C, 1C, 5C, etc.); and voltage window selection. During the experiments, rotary evaporation and heating (in tube furnace or oil bath) were used together to achieve the intermediates or crude products; sand/salt bath sublimation, soxhlet extraction, and recrystallization were tried to achieve the final products; thin layer chromatography (TLC), infrared spectroscopy (IR), nuclear magnetic resonance (NMR), scanning electron microscope (SEM), and x-ray diffraction (XRD) technique were used for characterizing crude/final product; heat treatment and acid treatment were used for carbon paper.

Further research is still needed to improve both yield and electrochemical properties of the materials, such as capacity, energy density, and cyclability. For PDI-based materials, more effort is needed to study the inner structure and how the process works when cycling and find the key reason leading to the bad performance.

Bibliography

- [1] J. Goldemberg, *World Energy Assessment: Energy and the Challenge of Sustainability*: United Nations Pubns, 2000.
- [2] D. Linden and T. B. Reddy, “Handbook of Batteries,” ed: McGraw-Hill Companies, Inc., 1865.
- [3] M. Winter and R. J. Brodd, “What Are Batteries, Fuel Cells, and Supercapacitors?,” *Chemical Reviews*, vol. 104, pp. 4245-4270, 2004.
- [4] D. Downs and A. Meyerhoff, “Battery, Baghdad, 250 BCE,” *Smith College*, vol. 22, 2000.
- [5] M. Piccolino, “Animal Electricity and the Birth of Electrophysiology: The Legacy of Luigi Galvani,” *Brain research bulletin*, vol. 46, pp. 381-407, 1998.
- [6] W. B. Jensen, “The Daniell Cell,” *Museum Notes*, 2013.
- [7] A. Boulabiar, K. Bouraoui, M. Chastrette, and M. Abderrabba, “A Historical Analysis of the Daniell Cell and Electrochemistry Teaching in French and Tunisian Textbooks,” *Journal of Chemical Education*, vol. 81, p. 754, 2004.
- [8] S. Karunathilaka, N. Hampson, T. Haas, R. Leek, and T. Sinclair, “The Impedance of the Alkaline Zinc-Mercuric Oxide Cell. I. Cell Behaviour and Interpretation of Impedance Spectra,” *Journal of Applied Electrochemistry*, vol. 11, pp. 573-582, 1981.
- [9] M. S. Whittingham, “Electrical Energy Storage and Intercalation Chemistry,” *Science*, vol. 192, pp. 1126-1127, 1976.

- [10] M. S. Whittingham, "Chemistry of Intercalation Compounds: Metal Guests in Chalcogenide Hosts," *Progress in Solid State Chemistry*, vol. 12, pp. 41-99, 1978.
- [11] K. Mizushima, P. Jones, P. Wiseman, and J. B. Goodenough, " Li_xCoO_2 ($0 < x \leq 1$): A New Cathode Material for Batteries of High Energy Density," *Materials Research Bulletin*, vol. 15, pp. 783-789, 1980.
- [12] D. Murphy and P. Christian, "Solid State Electrodes for High Energy Batteries," *Science*, vol. 205, pp. 651-656, 1979.
- [13] C. C. Lin, H. C. Wu, J. P. Pan, C. Y. Su, T. H. Wang, H. S. Sheu, and N. L. Wu, "Investigation on Suppressed Thermal Runaway of Li-Ion Battery by Hyper-Branched Polymer Coated on Cathode," *Electrochimica Acta*, vol. 101, pp. 11-17, Jul 1 2013.
- [14] B. J. Landi, M. J. Ganter, C. D. Cress, R. A. DiLeo, and R. P. Raffaele, "Carbon Nanotubes for Lithium Ion Batteries," *Energy & Environmental Science*, vol. 2, pp. 638-654, 2009.
- [15] J. M. Tarascon and M. Armand, "Issues and Challenges Facing Rechargeable Lithium Batteries," *Nature*, vol. 414, pp. 359-367, Nov 15 2001.
- [16] E. Stura and C. Nicolini, "New Nanomaterials for Light Weight Lithium Batteries," *Analytica Chimica Acta*, vol. 568, pp. 57-64, May 24 2006.
- [17] S. H. Ng, J. Wang, D. Wexler, K. Konstantinov, Z. P. Guo, and H. K. Liu, "Highly Reversible Lithium Storage in Spheroidal Carbon-Coated Silicon Nanocomposites as Anodes for Lithium-Ion Batteries," *Angewandte Chemie International Edition*, vol. 45, pp. 6896-6899, 2006.

- [18] S. Flandrois and B. Simon, "Carbon Materials for Lithium-Ion Rechargeable Batteries," *Carbon*, vol. 37, pp. 165-180, 1999.
- [19] M. Liang and L. Zhi, "Graphene-Based Electrode Materials for Rechargeable Lithium Batteries," *Journal of Materials Chemistry*, vol. 19, p. 5871, 2009.
- [20] N. Loeffler, D. Bresser, and S. Passerini, "Secondary Lithium-Ion Battery Anodes: From First Commercial Batteries to Recent Research Activities," *Johnson Matthey Technology Review*, vol. 59, pp. 34-44, 2015.
- [21] C. de las Casas and W. Li, "A Review of Application of Carbon Nanotubes for Lithium Ion Battery Anode Material," *Journal of Power Sources*, vol. 208, pp. 74-85, 2012.
- [22] D. Larcher, S. Beattie, M. Morcrette, K. Edstroem, J. C. Jumas, and J. M. Tarascon, "Recent Findings and Prospects in the Field of Pure Metals as Negative Electrodes for Li-Ion Batteries," *Journal of Materials Chemistry*, vol. 17, pp. 3759-3772, 2007.
- [23] J. Besenhard, M. Hess, and P. Komenda, "Dimensionally Stable Li-Alloy Electrodes for Secondary Batteries," *Solid State Ionics*, vol. 40, pp. 525-529, 1990.
- [24] P. Poizot, S. Laruelle, S. Grugeon, L. Dupont, and J. Tarascon, "Nano-Sized Transition-Metal Oxides as Negative-Electrode Materials for Lithium-Ion Batteries," *Nature*, vol. 407, pp. 496-499, 2000.
- [25] M. S. Whittingham, "Lithium Batteries and Cathode Materials," *Chemical reviews*, vol. 104, pp. 4271-4302, 2004.

- [26] A. Manthiram, A. V. Murugan, A. Sarkar, and T. Muraliganth, "Nanostructured Electrode Materials for Electrochemical Energy Storage and Conversion," *Energy & Environmental Science*, vol. 1, pp. 621-638, 2008.
- [27] K. Xu, "Non-aqueous Liquid Electrolytes for Lithium-Based Rechargeable Batteries," *Chemical reviews*, vol. 104, pp. 4303-4418, 2004.
- [28] W. A. Barber, A. M. Feldman, and A. V. Fraioli, "Composite Paper Electrode for a Voltaic Cell," ed: Google Patents, 1970.
- [29] J. R. Moser and A. A. Schneider, "Primary Cells and Iodine Containing Cathodes Therefor," ed: Google Patents, 1972.
- [30] K. Brandt, "Historical Development of Secondary Lithium Batteries," *Solid State Ionics*, vol. 69, pp. 173-183, 1994.
- [31] N. S. Choi, Z. Chen, S. A. Freunberger, X. Ji, Y. K. Sun, K. Amine, G. Yushin, L. F. Nazar, J. Cho, and P. G. Bruce, "Challenges Facing Lithium Batteries and Electrical Double-Layer Capacitors," *Angew Chem Int Ed Engl*, vol. 51, pp. 9994-10024, Oct 1 2012.
- [32] W. Li, J. R. Dahn, and D. S. Wainwright, "Rechargeable Lithium Batteries with Aqueous-Electrolytes," *Science*, vol. 264, pp. 1115-1118, May 20 1994.
- [33] J. Glanz, "Lithium Battery Takes to Water – and Maybe the Road," *Science*, vol. 264, pp. 1084-1084, May 20 1994.
- [34] J. Kohler, H. Makihara, H. Uegaito, H. Inoue, and M. Toki, "LiV₃O₈: Characterization as Anode Material for an Aqueous Rechargeable Li-Ion Battery System," *Electrochimica Acta*, vol. 46, pp. 59-65, Oct 31 2000.

- [35] W. Tang, Y. Zhu, Y. Hou, L. Liu, Y. Wu, K. P. Loh, H. Zhang, and K. Zhu, "Aqueous Rechargeable Lithium Batteries as an Energy Storage System of Superfast Charging," *Energy & Environmental Science*, vol. 6, p. 2093, 2013.
- [36] A. G. Macdiarmid, S. L. Mu, N. L. D. Somasiri, and W. Wu, "Electrochemical Characteristics of "Polyaniline" Cathodes and Anodes in Aqueous Electrolytes," *Molecular Crystals and Liquid Crystals*, vol. 121, pp. 187-190, 1985.
- [37] J. Y. Luo, W. J. Cui, P. He, and Y. Y. Xia, "Raising the Cycling Stability of Aqueous Lithium-Ion Batteries by Eliminating Oxygen in the Electrolyte," *Nat Chem*, vol. 2, pp. 760-765, Sep 2010.
- [38] C. Wessells, R. Ruffo, R. A. Huggins, and Y. Cui, "Investigations of the Electrochemical Stability of Aqueous Electrolytes for Lithium Battery Applications," *Electrochemical and Solid-State Letters*, vol. 13, pp. A59-A61, May 1, 2010 2010.
- [39] H. Kim, J. Hong, K. Y. Park, H. Kim, S. W. Kim, and K. Kang, "Aqueous Rechargeable Li and Na Ion Batteries," *Chem Rev*, vol. 114, pp. 11788-11827, Dec 10 2014.
- [40] M. Manickam, P. Singh, S. Thurgate, and K. Prince, "Redox Behavior and Surface Characterization of LiFePO₄ in Lithium Hydroxide Electrolyte," *Journal of Power Sources*, vol. 158, pp. 646-649, 2006.
- [41] C. D. Wessells, S. V. Peddada, M. T. McDowell, R. A. Huggins, and Y. Cui, "The Effect of Insertion Species on Nanostructured Open Framework Hexacyanoferrate Battery Electrodes," *Journal of The Electrochemical Society*, vol. 159, p. A98, 2012.

- [42] H. Manjunatha, G. S. Suresh, and T. V. Venkatesha, "Electrode Materials for Aqueous Rechargeable Lithium Batteries," *Journal of Solid State Electrochemistry*, vol. 15, pp. 431-445, 2010.
- [43] M. Thackeray, W. David, P. Bruce, and J. Goodenough, "Lithium Insertion into Manganese Spinel," *Materials Research Bulletin*, vol. 18, pp. 461-472, 1983.
- [44] J. Goodenough, M. Thackeray, W. David, and P. Bruce, "Lithium Insertion/Extraction Reactions with Manganese Oxides," *Revue de Chimie minerale*, vol. 21, pp. 435-455, 1984.
- [45] W. David, M. Thackeray, P. Bruce, and J. Goodenough, "Lithium Insertion into β -MnO₂ and the Rutile-Spinel Transformation," *Materials research bulletin*, vol. 19, pp. 99-106, 1984.
- [46] B. Xu, D. Qian, Z. Wang, and Y. S. Meng, "Recent Progress in Cathode Materials Research for Advanced Lithium Ion Batteries," *Materials Science and Engineering: R: Reports*, vol. 73, pp. 51-65, 2012.
- [47] Q. Qu, L. Fu, X. Zhan, D. Samuelis, J. Maier, L. Li, S. Tian, Z. Li, and Y. Wu, "Porous LiMn₂O₄ as Cathode Material with High Power and Excellent Cycling for Aqueous Rechargeable Lithium Batteries," *Energy & Environmental Science*, vol. 4, p. 3985, 2011.
- [48] G. J. Wang, Q. T. Qu, B. Wang, Y. Shi, S. Tian, Y. P. Wu, and R. Holze, "Electrochemical Behavior of LiCoO₂ in a Saturated Aqueous Li₂SO₄ Solution," *Electrochimica Acta*, vol. 54, pp. 1199-1203, 2009.

- [49] R. Ruffo, C. Wessells, R. A. Huggins, and Y. Cui, "Electrochemical Behavior of LiCoO_2 as Aqueous Lithium-Ion Battery Electrodes," *Electrochemistry communications*, vol. 11, pp. 247-249, 2009.
- [50] W. Tang, L. L. Liu, S. Tian, L. Li, Y. B. Yue, Y. P. Wu, S. Y. Guan, and K. Zhu, "Nano- LiCoO_2 as Cathode Material of Large Capacity and High Rate Capability for Aqueous Rechargeable Lithium Batteries," *Electrochemistry Communications*, vol. 12, pp. 1524-1526, 2010.
- [51] G. Wang, L. Fu, N. Zhao, L. Yang, Y. Wu, and H. Wu, "An Aqueous Rechargeable Lithium Battery with Good Cycling Performance," *Angew Chem Int Ed Engl*, vol. 46, pp. 295-297, 2007.
- [52] H. Wang, Y. Zeng, K. Huang, S. Liu, and L. Chen, "Improvement of Cycle Performance of Lithium Ion Cell $\text{LiMn}_2\text{O}_4/\text{Li}_x\text{V}_2\text{O}_5$ with Aqueous Solution Electrolyte by Polypyrrole Coating on Anode," *Electrochimica Acta*, vol. 52, pp. 5102-5107, 2007.
- [53] J. Y. Luo and Y. Y. Xia, "Aqueous Lithium-Ion Battery $\text{LiTi}_2(\text{PO}_4)_3/\text{LiMn}_2\text{O}_4$ with High Power and Energy Densities as Well as Superior Cycling Stability," *Advanced Functional Materials*, vol. 17, pp. 3877-3884, 2007.
- [54] D. Williams, J. Byrne, and J. Driscoll, "A High Energy Density Lithium/Dichloroisocyanuric Acid Battery System," *Journal of The Electrochemical Society*, vol. 116, pp. 2-4, 1969.
- [55] T. Nokami, T. Matsuo, Y. Inatomi, N. Hojo, T. Tsukagoshi, H. Yoshizawa, A. Shimizu, H. Kuramoto, K. Komae, H. Tsuyama, and J. Yoshida, "Polymer-Bound

- Pyrene-4,5,9,10-Tetraone for Fast-Charge and -Discharge Lithium-Ion Batteries with High Capacity,” *J Am Chem Soc*, vol. 134, pp. 19694-19700, Dec 5 2012.
- [56] Z. Song, H. Zhan, and Y. Zhou, “Anthraquinone Based Polymer as High Performance Cathode Material for Rechargeable Lithium Batteries,” *Chem Commun (Camb)*, pp. 448-450, Jan 28 2009.
- [57] M. Liu, S. J. Visco, and L. C. De Jonghe, “Novel Solid Redox Polymerization Electrodes: All-Solid-State, Thin-Film, Rechargeable Lithium Batteries,” *Journal of The Electrochemical Society*, vol. 138, pp. 1891-1895, 1991.
- [58] N. Oyama, T. Tatsuma, T. Sato, and T. Sotomura, “Dimercaptan–Polyaniline Composite Electrodes for Lithium Batteries with High Energy Density,” *Letters to Nature*, vol. 373, pp. 598-600, Feb 16 1995.
- [59] K. Naoi, K. Kawase, and Y. Inoue, “A New Energy Storage Material: Organosulfur Compounds Based on Multiple Sulfur-Sulfur Bonds,” *Journal of the Electrochemical Society*, vol. 144, pp. L170-L172, 1997.
- [60] W. Choi, D. Harada, K. Oyaizu, and H. Nishide, “Aqueous Electrochemistry of Poly(Vinylanthraquinone) for Anode-Active Materials in High-Density and Rechargeable Polymer/Air Batteries,” *J Am Chem Soc*, vol. 133, pp. 19839-43, Dec 14 2011.
- [61] Z. Song, H. Zhan, and Y. Zhou, “Polyimides: Promising Energy-Storage Materials,” *Angew Chem Int Ed Engl*, vol. 49, pp. 8444-8448, Nov 2 2010.
- [62] H. Qin, Z. P. Song, H. Zhan, and Y. H. Zhou, “Aqueous Rechargeable Alkali-Ion Batteries with Polyimide Anode,” *Journal of Power Sources*, vol. 249, pp. 367-372, 2014.

- [63] Y. Liang, P. Zhang, S. Yang, Z. Tao, and J. Chen, "Fused Heteroaromatic Organic Compounds for High-Power Electrodes of Rechargeable Lithium Batteries," *Advanced Energy Materials*, vol. 3, pp. 600-605, 2013.
- [64] Y. Liang, P. Zhang, and J. Chen, "Function-Oriented Design of Conjugated Carbonyl Compound Electrodes for High Energy Lithium Batteries," *Chemical Science*, vol. 4, p. 1330, 2013.
- [65] Y. Liang, Z. Tao, and J. Chen, "Organic Electrode Materials for Rechargeable Lithium Batteries," *Advanced Energy Materials*, vol. 2, pp. 742-769, 2012.
- [66] Y. Xu and Q. Zhang, "Two-Dimensional Fourier Transform Infrared (FT-IR) Correlation Spectroscopy Study of the Imidization Reaction from Polyamic Acid to Polyimide," *Appl Spectrosc*, vol. 68, pp. 657-62, 2014.
- [67] G. A. Mabbott, "An Introduction to Cyclic Voltammetry," *Journal of Chemical Education*, vol. 60, p. 697, 1983.
- [68] J. Heinze, "Cyclic Voltammetry – "Electrochemical Spectroscopy"," *Angewandte Chemie International Edition in English*, vol. 23, pp. 831-847, 1984.

